# Contribution of neuroplasticity in the insular cortex induced by nerve injury to neuropathic pain

Jeongsoo Han

Department of Medical Science

The Graduate School, Yonsei University

# Contribution of neuroplasticity in the insular cortex induced by nerve injury to neuropathic pain

Directed by Professor Bae Hwan Lee

The Doctoral Dissertation

submitted to the Department of Medical Science,

the Graduate School of Yonsei University

in partial fulfillment of the requirements for the degree of

Doctor of Philosophy

Jeongsoo Han

June 2017

This certifies that the Doctoral Dissertation of Jeongsoo Han is approved.

---

Thesis Supervisor : Bae Hwan Lee

---

Thesis Committee Member#1 : Jeong-Hoon Kim

---

Thesis Committee Member#2 : Insop Shim

---

Thesis Committee Member#3 : Chul Hoon Kim

---

Thesis Committee Member#4 : Jinwoong Bok

The Graduate School

Yonsei University

June 2017

# TABLE OF CONTENS

ABSTRACT ····· 1

I. INTRODUCTION ····· 4

II. STUDY 1. Changes of excitability of the insular cortex after nerve injury ····· 8

1. Purpose of the study ····· 8

2. Materials and methods ····· 9

A. Animals ····· 9

B. Neuropathic surgery ····· 9

C. Behavioral test for mechanical allodynia ····· 9

D. In vivo optical imaging ····· 10

E. Electrical stimulation ····· 11

F. Data analysis ····· 11

3. Results ····· 13

A. Development of neuropathic pain ····· 13

B. Representative spatiotemporal patterns of optical signals ····· 14

C. Optical signals in response to different intensities of electrical stimulation ····· 14

D. Quantitative analysis of changes in optical signals after nerve injury ····· 18

III. STUDY 2. PKMζ-related plastic changes in the IC after nerve injury ····· 20

1. Purpose of the study ····· 20

2. Materials and methods ····· 21
A. Animals ····· 21
B. Neuropathic surgery ····· 21
C. Behavioral test for mechanical allodynia ····· 21
D. Immunofluorescence double staining ····· 22
E. Immunohistochemistry ····· 23
F. Western blotting ····· 24
G. Statistical analysis ····· 25

3. Results ····· 26
A. Development of neuropathic pain ····· 26
B. Immunofluorescence double labeling of zif268 and NeuN ····· 27
C. Immunohistochemistry of zif268 in the insular cortex ····· 29
D. PKMζ and p-PKMζ expression level after nerve injury ····· 30
E. GluR1 and GluR2 expression level after nerve injury ····· 32

IV. STUDY 3. Modulation of the neuropathic pain by inhibition of PKMζ ····· 34
1. Purpose of the study ····· 34
2. Materials and methods ····· 35
A. Animals ····· 35
B. Cannulation and neuropathic surgery ····· 35
C. ZIP microinjection into the insular cortex, and analgesia test ····· 35
D. Western blotting ····· 36
E. Statistical analysis ····· 37

3. Results ····· 38

A. ZIP injection into the insular cortex ····· 38

B. Effects on PKMζ and p-PKMζ expression of ZIP microinjection into the insular cortex ····· 41

C. Effects of ZIP microinjection into the insular cortex on GluR1 and GluR2 levels ····· 43

V. DISCUSSION ····· 45

VI. CONCLUSIONS ····· 51

REFERENCES ····· 52

ABSTRACT (IN KOREAN) ····· 60

PUBLICATION LIST ····· 63

# LIST OF FIGURES

Figure 1. Development of mechanical allodynia after nerve injury ····· 13

Figure 2. Representative optical images of the IC in response to electrical stimulation ····· 15

Figure 3. Sequential images and time course of optical signals ····· 16

Figure 4. Comparison of optical intensity and activated area in sham and neuropathic rats one week after nerve injury ····· 19

Figure 5. Development of mechanical allodynia after nerve injury ····· 26

Figure 6. Immunofluorescence double labeling of zif268 and NeuN ····· 28

Figure 7. Immunohistochemistry of zif268 in the insular cortex ····· 29

Figure 8. Expression levels of PKMζ and p-PKMζ after nerve injury on POD 3····· 30

Figure 9. Expression levels of PKMζ and p-PKMζ after nerve injury on POD 7 ····· 31

Figure 10. Expression levels of GluR1 and GluR2 after nerve injury on POD 3 ····· 32

Figure 11. Expression levels of GluR1 and GluR2 after nerve injury on POD 7 ····· 33

Figure 12. Reduction of mechanical allodynia after ZIP microinjection into the IC ····· 39

Figure 13. Expression levels of PKMζ and p-PKMζ after ZIP microinjection into the IC on POD 3 ····· 41

Figure 14. Expression levels of PKMζ and p-PKMζ after ZIP microinjection into the IC on POD 7 ····· 42

Figure 15. Expression levels of GluR1 and GluR2 after ZIP microinjection into the IC on POD 3 ····· 43

Figure 16. Expression levels of GluR1 and GluR2 after ZIP microinjection into the IC on POD 7 ····· 44

<ABSTRACT>

**Contribution of neuroplasticity in the insular cortex induced by nerve injury to neuropathic pain**

Jeongsoo Han

*Department of Medical Science*

*The Graduate School, Yonsei University*

(Directed by Professor Bae Hwan Lee)

The insular cortex (IC) has been conventionally known to be involved in taste sensation. According to recent evidence, IC may play a role in diverse functions related to pain, emotion, and the regulation of the homeostasis. The IC is a pain-related brain region that receives various types of sensory input and processes the emotional aspects of pain. Peripheral nerve injury can induce neural plasticity of pain pathways including the IC that may contribute to chronic pain. However, there is no systematic report which studied the relationship between neuroplasticity and pain modulation after nerve injury in the IC. Therefore, this study was conducted to observe plastic changes in the IC after nerve injury and alleviation of pain by modulating these changes. Firstly, the optical imaging study was conducted to investigate spatiotemporal patterns related to neuroplastic

changes in the IC after nerve injury using voltage-sensitive dye imaging. The tibial and sural nerves of rats were injured under pentobarbital anesthesia. To observe optical signals in the IC, rats were re-anesthetized with urethane on post-operative day (POD) 7, and a craniectomy was performed for optical imaging. Optical signals of the IC were elicited by peripheral electrical stimulation. Neuropathic rats showed a significantly higher optical intensity following 5.0 mA electrical stimulation compared to sham-injured rats. A larger area of activation was observed by 1.25 and 2.5 mA electrical stimulation compared to sham-injured rats. The activated areas tended to be larger, and the peak amplitudes of optical signals were increased with increasing stimulation intensity in both groups. These results suggest that the elevated responsiveness of the IC to peripheral stimulation is related to neuropathic pain, and that neuroplastic changes are likely to be involved in the IC after nerve injury.

Secondly, the immunohistochemistry (IHC) and western blotting studies were conducted to observe protein kinase M ζ (PKMζ)-related plasticity of the IC after nerve injury. Continuous active kinase, PKMζ, has been known to maintain the late phase of long-term potentiation (L-LTP). Mechanical allodynia test and zif268 immunohistochemistry were performed after nerve injury. Zif268 have been to known as neuronal marker of plasticity and LTP. IHC was performed to test whether plasticity occur in the IC and the IC processes pain information. Zif268 expression level was significantly increased in the IC by nerve injury. Western blotting was conducted after nerve injury to assess expression of PKMζ phosphorylated-PKMζ (p-PKMζ) which is responsible in late-LTP. The results indicated that the expressions of PKMζ and p-PKMζ in the nerve-injured group on POD 3 tended to be increased than those of sham group, but showed no significant differences. The expression levels of PKMζ and p-PKMζ in the nerve-injured group on POD 7 were significantly increased than those of sham group.

The third study was conducted to determine the functional role of PKMζ which may be involved in the modulation of neuropathic pain IC. After ζ-pseudosubstrate inhibitory peptide (ZIP, a selective inhibitor of PKMζ) injection, mechanical withdrawal threshold and expression level of PKMζ, p-PKMζ, GluR1 and GluR2 were observed. Mechanical allodynia was significantly decreased by ZIP microinjection into the IC. The analgesic effect lasted for 12 hrs. Moreover, the levels of GluR1, GluR2, and p-PKMζ were decreased after ZIP microinjection. These results suggest that nerve injury induces plasticity related to PKMζ in the IC, and that the IC has a pain modulation function.

Taken together, these results suggest that the elevated responsiveness of the IC to peripheral stimulation is related to neuropathic pain, and that neuroplastic changes are involved in the IC after nerve injury. Furthermore, peripheral nerve injury induces neural plasticity related to PKMζ, and ZIP has potential applications for relieving chronic pain.

Key Words: insular cortex, nerve injury, neuropathic pain, neuroplasticity, optical imaging, voltage-sensitive dye, protein kinase Mζ

# Contribution of neuroplasticity in the insular cortex induced by nerve injury to neuropathic pain

Jeongsoo Han

*Department of Medical Science*

*The Graduate School, Yonsei University*

(Directed by Professor Bae Hwan Lee)

## I. INTRODUCTION

Chronic pain refers to prolonged pain that remains after recovery from peripheral nerve damage.[1] Recent studies have speculated that plastic changes induced by nerve injury in pain pathways may be the main cause of chronic pain.[1-4] A better understanding of the six brain areas related to pain processing that make up the pain matrix, namely, the anterior cingulate cortex, insular cortex (IC), primary somatosensory cortex (S1), secondary somatosensory cortex (S2), prefrontal cortex (PFC), and thalamus is important for treating chronic pain, since pain is both a subjective sensation and an emotional experience that requires integrated multidimensional processing in pain-related brain networks.[5-7] In fact, several studies have reported the existence of structural or functional plasticity in the ACC,[8,9] S1,[10] and PFC[11] in neuropathic and chronic pain models.

Although the IC was conventionally regarded as a gustatory cortex, it has been recently reported that the IC may play a critical role in processing and modulating pain sensation.[12-15]

Among the pain-related brain areas, the IC is one of the pain processing areas and is especially related to the emotional aspect of pain.[13,15-17] The conventional view of pain processing was that nociceptive information simply passes through the ventroposterior lateral nucleus of thalamus and then to the somatosensory cortex.[12] Recent functional imaging studies verified that ventromedial nucleus posterior part of thalamus projects the pain, temperature and interoceptive sensation to the dorsal IC.[12] Several human studies have provided insight into the pain-related functions of the IC. Specifically, lesions in this region cause pain asymbolia, a state in which a patient is able to recognize painful stimulus but does not avoid because the patient cannot interpret this stimulus as pain.[18] These patients did not display appropriate responses to pain, but all other sensory and cognitive functions still remained intact.[18] Human electrode recording and fMRI studies indicate that both acute and chronic pain result in activation of the IC, and also that direct stimulation of the IC can cause pain sensation.[12,19-22] Painful stimuli activate the IC, and direct stimulation of the IC can evoke sensations of pain, indicating that the IC is pronociceptive and is involved in the interpretation of pain sensation.[13,19,20] Patient's with irritable bowel syndrome accompanying hyperalgesia exhibit increased activity of the IC and ACC.[23] Likewise, an EEG study reported that patients suffering from chronic neurogenic pain showed enhanced spontaneous activity, such as high and low theta frequencies, in pain matrix areas including the IC compared to healthy individuals.[24]

In addition, many animal studies demonstrate the function of the IC related to pain processing and modulation. Numerous recent reports have suggested that the plasticity of pain-related brain areas contributes to chronic pain states.[1] Animals with lesions of the IC

show reversed neuropathic or inflammatory pain behavior, but did not affect non-nociceptive mechanical thresholds..[25,26] Jasmin et al.[13,15] showed that the IC has a key role in pain information processing and pain modulation by changing the pain threshold using GABA neurotransmission. Nevertheless, there are relatively few studies about nerve injury-related plastic changes in the IC and their contribution to chronic pain.

Optical imaging using voltage-sensitive dyes is a functional brain imaging technique that enables visualization of neuronal activity of large populations and changes in membrane potential.[27] Owing to the high spatiotemporal resolution of this technique, several studies have reported excitatory propagation patterns in several brain areas.[28-32] For example, an optical imaging study reported that the cortical excitability of the S1 is modified following nerve injury.[33] However, there has been no report on functional plastic changes in the rat IC after nerve injury using in vivo optical imaging.

Nerve injury-induced neural plasticity within the central nervous system is one of the important mechanisms for chronic pain.[1,3,4,34] Long-term potentiation (LTP) is underlying mechanism of synaptic plasticity and is thought as the neural substrate of learning and memory.[35,36] Furthermore, several studies have reported LTP is induced by pain in the spinal cord and cortex both in the acute chronic pain states.[8,37,38] Thus, it is believed that there are common mechanism between learning/memory and chronic pain.[39]

Protein kinase M zeta (PKMζ) is a key molecule required for maintenance of late LTP (L-LTP).[40,41] It is one of the atypical PKC isoforms as PKMζ, PKCζ, PKCλ. Because PKMζ has only catalytic domain of PKCζ, lacking regulatory domain, it can be persistently activated.[42] In fact, NMDA receptor-dependent plastic change including LTP after nerve injury and PKMζ-mediated conditioned taste aversion (CTA) memory of the IC has been reported.[43,44] But there is no study about LTP biomarker and PKMζ-related mechanism of plasticity after nerve injury in the IC.

Zif268, also known as early growth response protein 1 (EGR-1), is required for consolidation of L-LTP in the hippocampus and the spinal cord.[45,46] In order to determine whether there is possibility of LTP induction in the IC after nerve injury, the zif268 level was observed in this study.

In rodents, lesions to the IC reverse neuropathic pain states to normal states, but do not affect non-nociceptive mechanical thresholds.[25,26] Jasmin et al.[13,15] showed that the IC has a key role in pain information processing and pain modulation. Zeta inhibitory peptide (ZIP), inhibitor of PKMζ, can reverse LTP maintenance and block the L-LTP formation.[47,48] Furthermore ZIP can also erase spatial, fear, addiction, and CTA memory involved in various CNS regions.[43,48-51] Recently, several studies reported that PKMζ-related pain memory can be erased in the spinal cord and brain.[8,52,53]

However, there is no systematic report which studied the relationship between neuroplasticity and pain modulation in IC. Therefore, the present study is to determine mechanisms which may be involved in neural plasticity and modulation of neuropathic pain in the IC after nerve injury, using convergent approaches.

## II. STUDY 1 : Changes of excitability in the IC after nerve injury

### 1. Purpose of the study

Optical imaging using voltage-sensitive dyes is a functional brain imaging technique that enables visualization of neuronal activity of large populations and changes in membrane potential.[27] Owing to the high spatiotemporal resolution of this technique, several studies have reported excitatory propagation patterns in several brain areas.[28-32] In fact, optical imaging study was used to reveal the plasticity of cortical excitability in the S1 following nerve injury.[33] However, there has been no report on functional plastic changes in the IC after nerve injury using in vivo optical imaging. Thus, the purpose of study 1 is to investigate excitatory patterns and changes related to neuroplasticity in the IC after nerve injury using optical imaging.

## 2. Materials and methods

### A. Animals

All experimental procedures in this study were conducted in accordance with the National Institute of Health guidelines and were approved by the Institutional Animal Care and Use Committee of the Yonsei University Health System. Male Sprague-Dawley rats (Koatec, Pyeongtaek, Korea, 180-200 g) were allowed to acclimate for a period of 7 days after arrival and accommodated in the temperature-controlled room with food pellets and water provided ad libitum.

### B. Neuropathic surgery

Under sodium pentobarbital (50 mg/kg, i.p.) anesthesia, branches of the left sciatic nerve were exposed by dissecting the skin and biceps femoris muscle. The tibial and sural nerves were tightly ligated and transected, while the common peroneal nerve was left intact.[54] Muscle and skin layers were sutured and a drop of lidocaine was applied to the wound. The sham control group underwent the same operation without any nerve damage.

### C. Behavioral test for mechanical allodynia

A mechanical threshold test was used to confirm the development of neuropathic pain. A blind test was conducted to observe the mechanical threshold on post-operative days (PODs) 1, 3, and 7. Rats were placed on an elevated metal mesh floor under rectangular-shaped transparent domes and familiarized to the test conditions for 15 mins. Mechanical withdrawal thresholds were assessed by applying an electronic von Frey filament (UGO

Basile, Varese, Italy) to the medial dorsal paw area of nerve-injured left hind paws. The mechanical withdrawal threshold was tested eight times, and the results excluding maximal and minimal values were averaged. The mechanical force was recorded when a positive withdrawal response of the hind paw occurred, defined as licking or flicking of the left paw.

D. In vivo optical imaging

Rats (sham and nerve injury group, n=5 and n=7 respectively) received dexamethasone sulfate (1 mg/kg, ip) one day before the optical imaging experiment to reduce swelling of the cortex. Seven days after nerve injury, rats were anesthetized with urethane (1.25 g/kg, i.p.) and given atropine (5 mg/kg, i.p.) to prevent mucus secretion. Rats were placed on their side in a custom-made stereotacxic frame such that they were lying in a lateral position, which afforded access to the IC located in the anterolateral aspect of the rat brain. An ophthalmic lubricant ointment was applied to both eyes to prevent desiccation. Heart rate was monitored by electrocardiography and body temperature was maintained at 36℃ with a rectal probe and heating pad system (Homeothermic Blanket Control Unit, Harvard Apparatus, Holliston, MA, USA). Prior to craniectomy, lidocaine was applied to the right temporal muscle and the skin contralateral to the nerve injury. Craniectomy was performed to visualize the IC after preparation steps. The skin overlying the temporalis muscle, the muscle, and zygomatic arch were carefully resected to prevent excessive bleeding. Finally, the cortex was stained using a voltage-sensitive dye (VSD; di-2-ANEPEQ, 50 μg/mL in saline, Molecular Probes, Eugene, OR, USA) after the dura was removed to expose the surface of the cortex. The cortex was carefully rinsed with saline one hr after staining.

The optical imaging method was performed as described in other studies.[33,55] Briefly, the imaging site was focused on the IC surface with the camera axis perpendicular to the IC. The fluorescence of the dye was detected using an optical imaging system consisting of a high resolution CCD camera (Brainvision Inc., Tokyo, Japan) equipped with a dichroic mirror with a 510–550 nm excitation filter and 590 nm absorption filter. A tungsten halogen lamp (150 W) was used for excitation of fluorescence. The imaging area was 6.4 x 4.8 $mm^2$ and consisted of 184 x 124 pixels.

E. Electrical stimulation

A pair of stainless steel electrodes was implanted in the peripheral receptive field of the left hind paw where the electronic von Frey filament was applied during behavioral testing. The receptive field was stimulated with a square pulse (width: 0.1 ms, interstimulus interval: 5 s, intensity: 0, 0.6, 1.25, 2.5, and 5.0 mA) using a stimulus isolation unit (World Precision Instruments, Sarasota, FL, USA). During each trial, the change in fluorescence intensity was measured for approximately 940 ms. The recording surface was placed under an optical microscope (Leica Microsystems Ltd., Heerbrugg, Switzerland) equipped with a 1× objective and 1× projection lens. Optical signals were acquired at a rate of 3.7 ms/frame and averaged 30 times using an optical imaging recording system (MiCAM02, Brainvision Inc.). Optical imaging acquisition was triggered by electrocardiogram signals using a stimulus/non-stimulus subtraction method. After optical imaging, rats were euthanized by over dose of urethane.

F. Data analysis

In order to normalize the value of each pixel, the ratio of the intensity of fluorescence (ΔF) in each pixel relative to the initial fluorescence intensity (F) was expressed as the fractional change (ΔF/F). Amplitudes and excitatory areas of optical signals were measured using a spatial filter (9 x 9 pixels) to reduce artifacts caused by vibration and brain movements. Data were collected and illustrated using BV Analyzer software (Brainvision Inc.).

Using captured images, fractional changes in optical signals (optical intensity) and areas of activation were quantified. Changes in optical intensity in the IC were determined as the ratio of change in the intensity of fluorescence (ΔF) to the initial intensity of fluorescence (F) expressed as percent fractional change (ΔF/F × 100). In order to analyze the area of activation, a region of interest (ROI) was delineated using a black dashed-line (circle of 20 pixel radius) as shown in Fig. 2A. The activated area was defined as the activated pixel number of the ROI / total pixel number of the ROI × 100. The optical intensity and the activated area were analyzed using BV Analyzer software (Brainvision Inc.).

Data are presented as the mean±standard error of the mean (SEM). Differences in intensities of optical signals and areas of activation were analyzed with unpaired t-tests. P values less than 0.05 were considered significant. Unpaired t-test for post-hoc comparison was used for two-group comparisons while two-way ANOVA with repeated measures was used to analyze behavioral test.

## 3. Results

A. Development of neuropathic pain

Mechanical allodynia was elicited by injuries of the two major branches (the sural and tibial nerves) of the sciatic nerve on PODs 1, 3, and 7 (Figure 1). The mechanical threshold of the nerve-injured group decreased on PODs 1, 3, and 7 relative to the sham group.

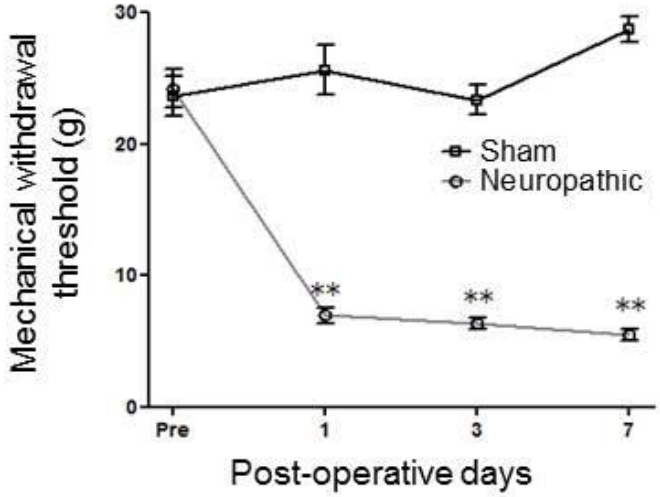


**Figure 1. Development of mechanical allodynia after nerve injury.** On PODs 1, 3, and 7, neuropathic rats (n=7) showed a significantly decreased mechanical withdrawal threshold compared to the sham-operated group (n=5, two-way ANOVA repeated measures $P < 0.01$, unpaired t-test, $^{**}P < 0.01$).

B. Representative spatiotemporal patterns of optical signals

To distinguish adjacent brain areas from the IC, the lateral view of the exposed cortex was delineated according to other reports (Figure 2A).[56,57] Representative optical images were obtained by electrical stimulation (1.25 mA) of the contralateral hind paw in sham and nerve-injured rats (Figure 2B and C). Images of the left column were color-coded to show optical signals induced by stimulation according to the fractional changes in reflected light intensity (%ΔF/F). Wave forms were used to show the optical responses at specific points in the ROI (red dots) of the IC. Whereas the IC of the sham-operated rats rarely showed a response, the IC of neuropathic rats was extensively activated in response to peripheral electrical stimulation (Figure 2C).

C. Optical signals in response to different intensities of electrical stimulation

A time course of optical signals induced by different intensities of electrical stimulation was used to show the differences between neuropathic and sham-operated rats (Figure 3). The color-coded activated area and wave forms of sham-operated and nerve-injured rats are shown in Figure 3A and 3B, respectively. Although activated signals were not detected in the IC of the sham group after 0.6 and 1.25 mA electrical stimulation, 1.25 mA stimulation led to activation in the nerve-injured group. Electrical stimulation intensity of 2.5 and 5.0 mA led to excitation in both sham-operated and nerve-injured rats. In addition, the nerve-injured rats exhibited a more extensive and longer duration of excitation than sham-operated rats. The S2 was obviously activated by electrical stimulation due to the way divisions of the body are represented in the sensory cortex, the so called ratunculus. However, activation in the S2 area was excluded from analysis because it was not included in the ROI.

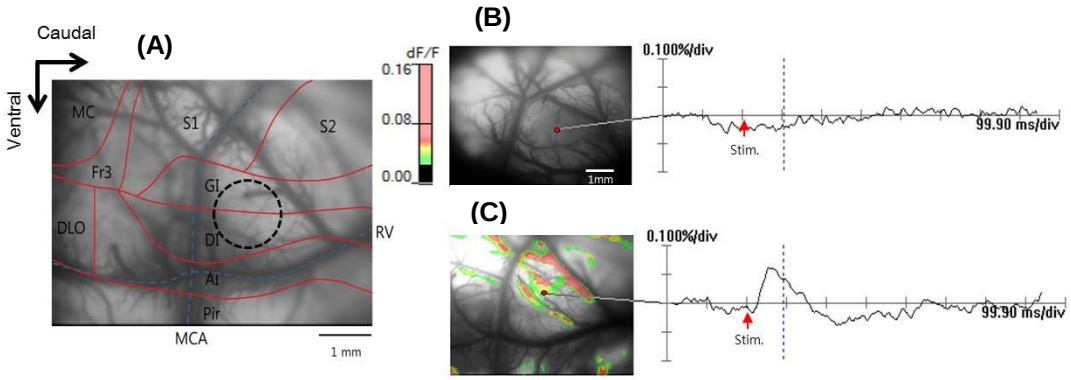


**Figure 2. Representative optical images of the IC in response to electrical stimulation of the hind paw (1.25 mA) in sham and nerve-injured groups.** (A) Location of the insular cortex. S1: primary somatosensory cortex, S2: secondary somatosensory cortex, GI: granular insular cortex, DI: dysgranular insular cortex, AI: agranular insular cortex, Pir: piriform cortex, MC: motor cortex, DLO: dorsolateral orbital cortex, Fr3: frontal cortex area 3, RV: rhinal vein, MCA: middle cerebral artery. The black dashed line represents the ROI of the IC. (B) Optical image from a sham rat. (C) Optical image from a nerve-injured rat. The activated cortical area was color-coded, and the data from optical images was expressed as the percent change in fluorescent intensity (%ΔF/F). Each optical image was obtained at 300 ms, and each optical signal in the right panel was obtained at the red point in the corresponding left image.

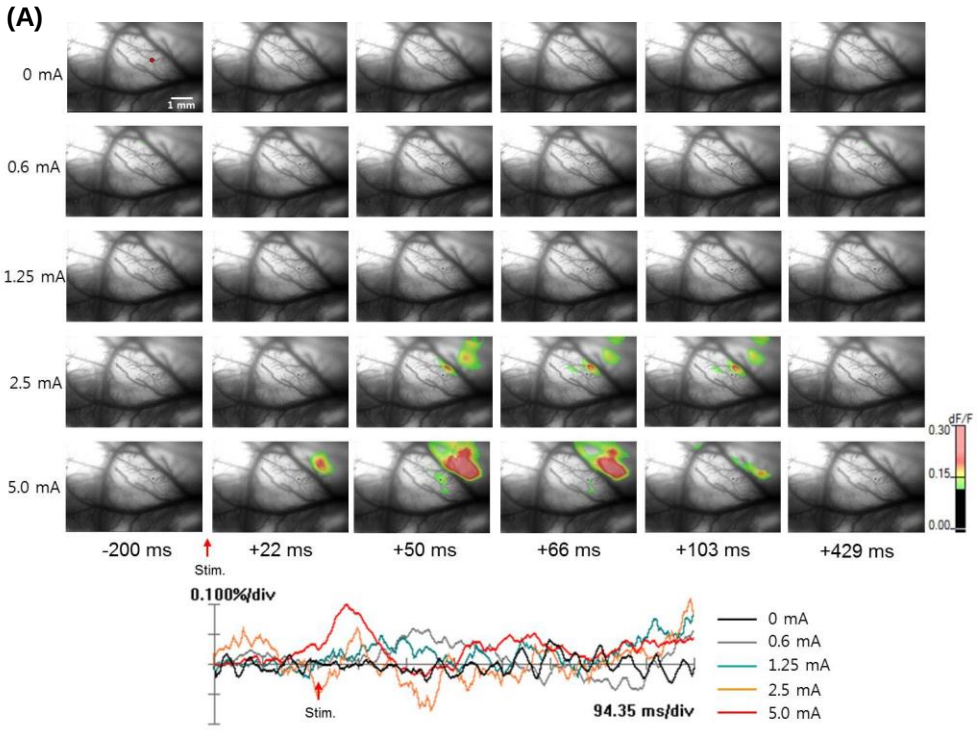


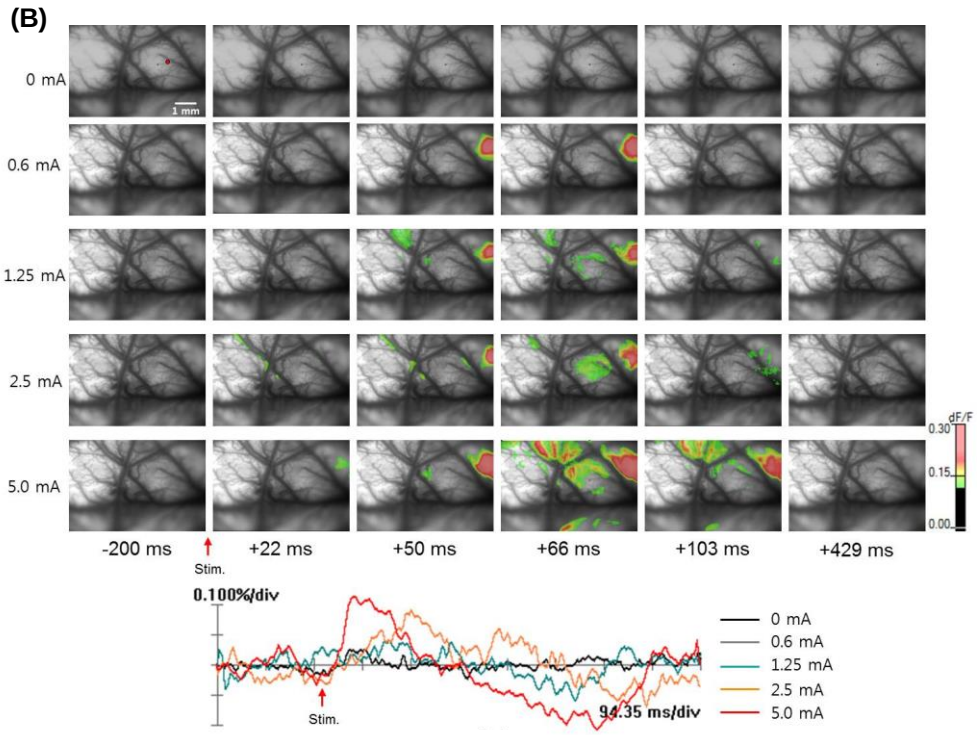

**Figure 3. Sequential images and time course of optical signals in sham (A) and neuropathic (B) rats.** Optical signals were induced using different intensities of electrical stimulation to the hind paw in sham and neuropathic rats. Electrical stimulation was applied to the hind paw at 0 ms (red arrow). Lower panels of both (A) and (B) represent the wave forms of optical signals activated by different intensities of electrical stimulation. S2 was obviously activated in the hind paw area of the ratunculus by peripheral electrical stimulation, but excluded from analysis because it was not in the ROI.

D. Quantitative analysis of changes in optical signals after nerve injury

Peak amplitudes and the activated area are represented in Figure 4A and 4B, respectively. The peak amplitude evoked by 5.0 mA electrical stimulation of nerve-injured rats was increased compared to sham-operated rats (Figure 4A, $P < 0.05$). The activated area evoked by 1.25 and 2.5 mA electrical stimulation in nerve-injured rats was also increased compared to sham-operated rats (Figure 4B, $P < 0.05$). On the other hand, there was no significant difference between nerve-injured and sham groups following 5.0 mA stimulation. These results suggest that peak amplitude is more sensitive to high stimulation intensity and that the activation area is likely to become saturated at relatively low stimulation intensities. Sham-operated and neuropathic rats tended to exhibit increased amplitude and activated area following electrical stimulation at different intensities ranging from 0.6 to 5.0 mA. In addition, neuropathic rats displayed more sensitive response to increasing stimulation intensities (Figure 4A and B).

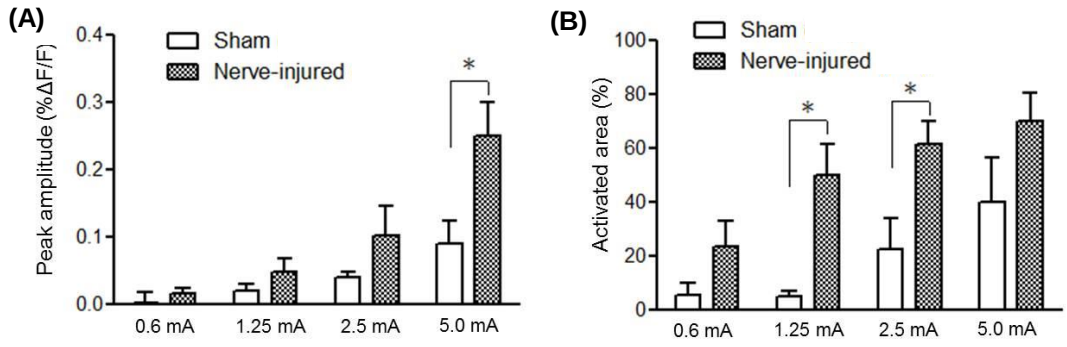


**Figure 4. Comparison of optical intensity and activated area in sham and neuropathic rats one week after nerve injury.** (A) Optical intensity in the IC induced by 5.0 mA electrical stimulation of the peripheral receptive field was significantly increased 1 week after nerve injury (n=7) compared to sham injury (n=5). (B) The size of the area activated by 1.2 and 2.5 mA electrical stimulation of the peripheral receptive field was also significantly increased 1 week after nerve injury (n=7) compared to sham injury (n=5, *$P < 0.05$). However, there was no significant difference in the area activated by 5.0 mA stimulation.

## III. STUDY 2 : PKMζ-related plastic changes in the IC after nerve injury

### 1. Purpose of the study

PKMζ is a key molecule required for maintenance of late LTP (L-LTP).[40,41] It is one of the atypical PKC isoforms as PKMζ, PKCζ, PKCλ. Because PKMζ has only catalytic domain of PKCζ, lacking regulatory domain, it can be persistently activated.[42] In fact, NMDA receptor-dependent plastic changes including LTP after nerve injury in the IC and PKMζ-mediated CTA memory has been reported.[43,44] But there is no study about LTP biomarker and PKMζ-related mechanism of plasticity in the IC after nerve injury.

Zif268 is required for consolidation of L-LTP in the hippocampus and the spinal cord.[45,46] In order to determine whether there is possibility of LTP induction in the IC after nerve injury, the immunohistochemical study was performed for zif268 also known as EGR-1. Moreover, to reveal role of PKMζ related to pain maintenance, the expression level of PKMζ, phosphor-PKMζ and AMPA receptor subunits were confirmed. Therefore, the purpose of the study 2 is to determine the PKMζ-related plastic changes in the IC related to LTP maintenance after nerve injury.

## 2. Materials and methods

### A. Animals

All experimental procedures in this study were conducted in accordance with the National Institute of Health guidelines and were approved by the Institutional Animal Care and Use Committee of the Yonsei University Health System. Male Sprague-Dawley rats (Koatec, Pyeongtaek, Korea, 180-200 g) were allowed to acclimate for a period of 7 days after arrival and were accommodated in the temperature-controlled room with food pellets and water provided ad libitum.

### B. Neuropathic surgery

Under sodium pentobarbital (50 mg/kg, i.p.) anesthesia, branches of the left sciatic nerve were exposed by dissecting the skin and biceps femoris muscle. The tibial and sural nerves were tightly ligated and transected, while the common peroneal nerve was left intact.[54] Muscle and skin layers were sutured and a drop of lidocaine was applied to the wound. The sham control group underwent the same operation without any nerve damage.

### C. Behavioral test for mechanical allodynia

A mechanical threshold test was used to confirm the development of neuropathic pain. A blind test was conducted to observe the mechanical threshold on PODs 1, 3, and 7. Rats were placed on an elevated metal mesh floor under rectangular-shaped transparent domes and familiarized to the test conditions for 15 mins. Mechanical withdrawal thresholds were assessed by applying an electronic von Frey filament (UGO Basile,

Varese, Italy) to the medial dorsal paw area of nerve-injured left hind paws. The mechanical withdrawal threshold was tested eight times, and the results excluding maximal and minimal values were averaged. The mechanical force was recorded when a positive withdrawal response of the hind paw occurred, defined as licking or flicking of the left paw.

D. Immunofluorescence double staining

For double immunofluorescence staining, rats were deeply anesthetized with urethane and perfused transcardially with saline followed by 4% paraformaldehyde in 0.1 M sodium phosphate buffer (PB, pH 6.8). The brain was removed from the skull and post-fixed with 4% paraformaldehyde in PB at 4℃ overnight. After post-fixation, the brain block was transferred into phosphate-buffered saline (PBS, pH 7.4) containing 30% sucrose for 24 hrs. The brain sample was covered with a cryo-section compound (frozen section compound FSC 22, Leica, Wetzlar, Germany) and was frozen in -70℃ deep freezer. Sample tissues were cut on a coronal section of 30 ㎛ thickness on a cryostat (HM 525, Thermo Scientific, Waltham, MA, USA). Section slides were then washed 3 times with 1X tris-buffered saline (TBS) containing 0.025% Triton X-100. After washing, the section slides were incubated in 10% normal goat serum (Vector Laboratories, Burlingame, CA, USA) with 1% bovine serum albumin (BSA, Thermo Scientific) in TBS for 1 hr at room temperature. The sections were incubated overnight in rabbit monoclonal anti-zif268 antibody (1:200, Santa Cruz Biotechnology, Santa Cruz, CA, USA) and mouse monoclonal anti-NeuN antibody (1:200, Abcam, Cambridge, UK) diluted in 10% normal goat serum with TBS containing 1% BSA at 4℃. The sections were then rinsed 2 times with 1X TBS plus 1% Tween-20. After washing 2 times for 10 mins, sections were incubated in secondary antibodies which were goat anti-rabbit Alexa Fluor 488 (1: 200,

Abcam) and goat anti-mouse Alexa Fluor 647 (1:200, Abcam), diluted in 10% normal goat serum with TBS containing 1% BSA for 1 hr at room temperature. Finally, the slides were washed 2 times with 1X TBS containing 0.025% Triton X-100 and mounted in Vectashield mounting media (Vector Laboratories).

E. Immunohistochemistry

To calculate the population of zif268-positive cells, 3,3' diaminobenzidine (DAB)-nickel immunostaining was performed on POD 3. Briefly, rat brain slices were prepared using the same steps as for immunofluorescence staining. For zif268 staining, section slides were rinsed 5 times with 1X PBS and incubated in methanol with 0.3% H2O2 for 15 mins to inhibit endogenous peroxidase activity. After washing the slides 5 times, the sections were incubated with PBS containing 1% normal horse serum (Vector Laboratories) for 30 mins and then incubated overnight at 4℃ in 0.3% Triton X-100, 2% normal horse serum (Vector Laboratories), and rabbit monoclonal anti-zif268 antibody (1:4,000, Santa Cruz Biotechnology). The sections were rinsed 5 times with 1X PBS and incubated for 30 mins in a universal biotinylated anti-mouse/rabbit secondary antibody (1:50, Vector Laboratories). Section slides were then washed again and incubated for 30 mins with PBS containing avidin-biotinylated horseradish peroxidase complex (1:50, Vector Laboratories). Following washing 5 times for 15 mins, sections were incubated for 5 mins in a solution containing 0.1% of DAB and 0.1% ammonium nickel sulfate in 1X PBS and 0.01% H2O2. Finally, the sections were washed to stop the DAB reaction, serially dehydrated in 50, 70, 95, and 100% ethanol, cleared in xylene, and coverslipped with permount (Fisher Scientific, Waltham, MA, USA).

To quantify zif268-positive cells in the IC, 8 representative sections of the IC were

chosen from each brain. The interval of each section was 300 ㎛. Therefore, 8 sections cover anteroposterior range (2.1 mm) of the IC. Zif268-positive cells in the IC were identified with reference to the brain atlas of Paxinos and Watson.[58] All of the zif268-labeled cells from light-field microscopy image (20x objective lens, Olympus BX40, Olympus, Tokyo, Japan) were counted manually. An experimenter blinded to the treatment conditions counted zif268-labeled cells of the ipsilateral and contralateral sides.

F. Western blotting

To collect insular cortices, animals were anesthetized with enflurane and decapitated. The ipsilateral and contralateral rostral insular cortices were quickly isolated and transferred into a deep freezer. Extracted samples were stored at -70℃. For protein extraction, samples were homogenized by sonication in lysis buffer (Proprep, iNtRON Biotechnology Inc, Seongnam, Korea) containing phosphatase inhibitor (PhosStop, Roche, Penzberg, Germany). Samples were centrifuged at 22,250 g for 10 mins at 4℃ and supernatants were collected, and total protein concentrations of lysates were assessed with a spectrophotometer (ND-1000, NanoDrop Technologies Inc, Wilmington, DE, USA). 10 μl of protein of brain tissue extracts was denatured per well and run on 10% Bis-Tris gels (Bio-Rad, Hercules, CA, USA) for detection of PKMζ, p-PKMζ, GluR1, and GluR2. Proteins were transferred onto polyvinylidene difluoride (PVDF) membranes (GE Healthcare, Buckinghamshire, UK). Membranes were blocked in 5% skim milk in TBS with Tween-20 for 1 hr and incubated in primary antibodies overnight on a rocking platform at 4℃. Primary antibodies against PKMζ (1:2,000, Cell Signaling Technology, Beverly, MA, USA), p-PKMζ (1:2,000, Cell Signaling Technology), GluR1 (1:2,000, Millipore, Temecula, MA, USA), GluR2 (1:2,000, Abcam), GAPDH (1:10,000, Ab Frontier, Seoul, Korea), β-actin (1:10,000, Cell Signaling Technology) were used for

western blotting. On the following day, the membranes were incubated in the appropriate secondary antibodies for 2 hrs and horseradish peroxidase activity was visualized using a chemiluminescent substrate (ECL™ Prime western blotting detection reagent, GE Healthcare) and processed with a local allocation system (LAS) system (ImageQuant LAS 4000 Mini, GE Healthcare). The intensity of the bands for PKMζ, GluR1 and GluR2 were normalized to the intensity of GAPDH or β-actin. The intensity of the bands for p-PKMζ was normalized to the intensity of PKMζ.

G. Statistical analysis

Unpaired t-test for post-hoc comparison was used for two-group comparisons while two-way ANOVA with repeated measures was used to analyze behavioral test. Western blots and IHC were compared using an unpaired t-test. All data were expressed as the mean ± SEM. A p-value less than 0.05 was considered statistically significant.

## 3. Results

A. Development of neuropathic pain

Mechanical allodynia was elicited by injuries of the two major branches (the sural and tibial nerves) of the sciatic nerve on PODs 1, 3, and 7 (Figure 5). The mechanical threshold of the nerve-injured group decreased on PODs 1, 3, and 7 relative to the sham group. (A) shows the mechanical withdrawal threshold of the nerve injury model and sham model for experiment on POD 3. (B) shows the mechanical withdrawal threshold of nerve injury model and sham model for experiment on POD 7

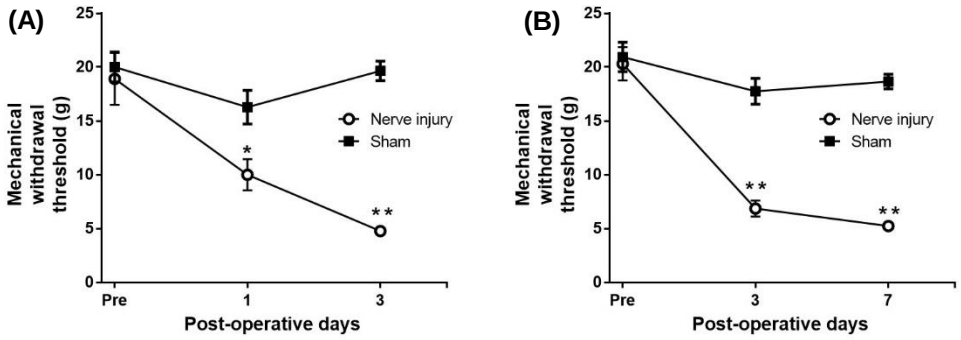


**Figure 5. Development of mechanical allodynia after nerve injury.** (A) On PODs 1, 3 neuropathic rats (n=6) showed a significantly decreased mechanical withdrawal threshold compared to the sham-operated group (n=6, two-way ANOVA repeated measures, $P < 0.01$, unpaired t-test, *$P < 0.05$, **$P < 0.01$). These animals was used for experiment on POD 3. (B) On PODs 3, 7 neuropathic rats (n=11) showed a significantly decreased mechanical withdrawal threshold compared to the sham-operated group (n=11, two-way ANOVA repeated measures $P < 0.01$, unpaired t-test, **$P < 0.01$). These animals was used for experiment on POD 7.

B. Immunofluorescence double labeling of zif268 and NeuN

To confirm that zif268 was co-expressed with NeuN in the IC, double labeling of zif268 and NeuN was performed. The representative images of the nerve-injured group are shown in Figures 6D, 6E, and 6F, and those of the sham group are shown in Figures 6A, 6B, and 6C. Zif268 immunoreactivity (green) was observed in the IC (Figures 6A and 6D). NeuN, a neuronal marker (red), was observed in the IC (Figures 6B and 6E). Colocalization of zif268 (green) and NeuN (red) was detected in the IC (Figures 6C and 6F). As shown in Figure 6, zif268-positive cells were colocalized with NeuN-positive cells. This result indicates that zif268 is expressed in IC neurons. Nerve-injured rats have more zif268-positive cells (Figure 6A) than the sham group rats (Figure 6D). The number of NeuN-positive cells in the IC is similar between the nerve-injured (Figure 6E) and sham-operated groups (Figure 6B). The merged data of zif268 and NeuN expression show that the IC has a relationship with neuropathic pain (Figures 6C and 6F).

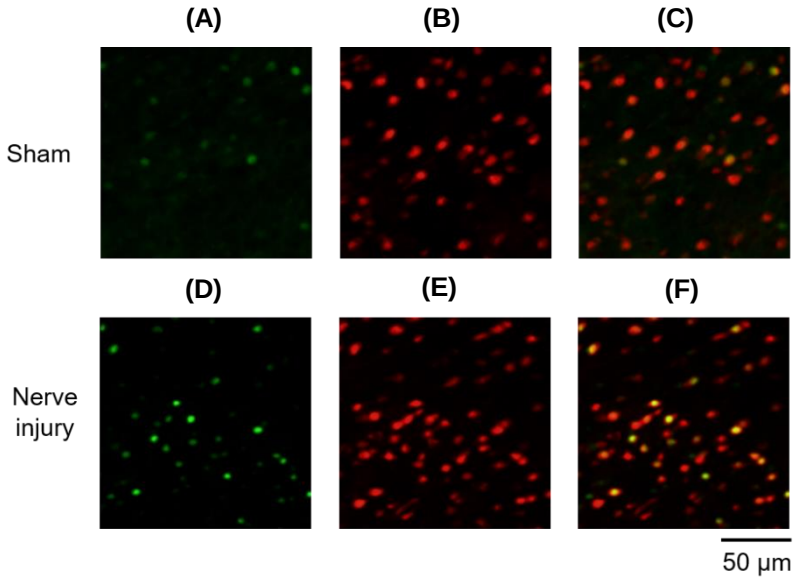


**Figure 6. Fluorescence images of zif268 expression in the IC of nerve-injured and sham groups.** (A) In the nerve-injured group, the distribution of zif268 expression (green) was denser than in the sham group. (B) The sham group showed little expression of zif268-positive cells, unlike the nerve-injured group. (C) NeuN, a neuronal marker (red), was expressed in the nerve-injured group. (D) As in (C), NeuN was expressed in the sham group. (E) Colocalization of zif268 (green) and NeuN (red) in the nerve-injured group. (F) As in (E), colocalization of zif268 (green) and NeuN (red) is observed in the sham group.

C. Immunohistochemistry of zif268 in the insular cortex

Zif268-positive cells were found in the IC of nerve-injured rats (Figures 7A and 7B). Furthermore, zif268 immunohistochemistry was performed to quantify the zif268-positive cells in the nerve-injured and sham groups. The results showed that the number of zif268-positive cells in the nerve-injured group was significantly increased than that of the sham group (Figure 7C, *P < 0.05).

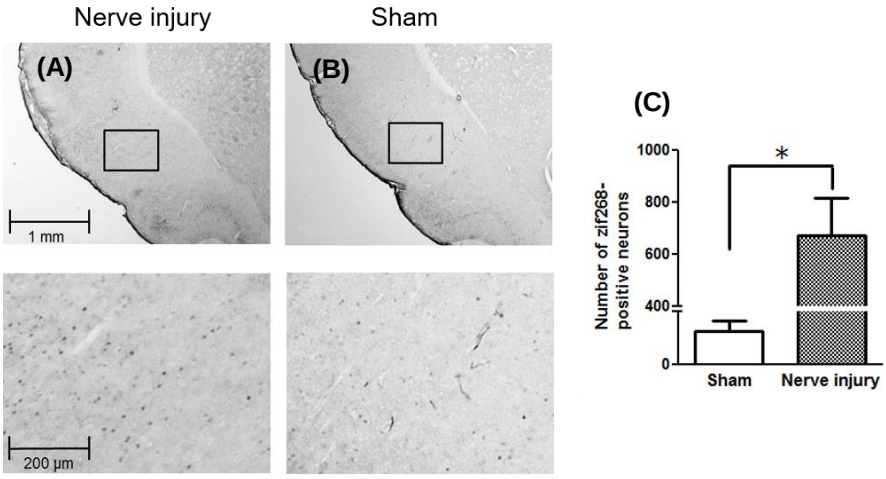


**Figure 7. Zif268-positive cells in the IC. (A) Zif268-positive cells in the IC of a nerve-injured rat.** (B) Zif268-positive cells in the IC of a sham-operated rat (n=6). (C) Comparison of zif268-positive cells in the nerve-injured and sham groups (n=6). Zif268-positive cells increased significantly in the IC after nerve injury (*P < 0.05). Cell counts are expressed per section.

D. PKMζ and p-PKMζ expression level after nerve injury

To determine whether the nerve injury can cause the plasticity-related molecular change, sample of the IC was punched on PODs 3 and 7. The total PKMζ in the neuropathic pain (NP) group was not changed (Figure 8A, $P > 0.05$) on POD 3 relative to the sham group. Similarly, the expression level of p-PKMζ was not changed by nerve injury on POD 3 (Figure 8B, $P > 0.05$). The PKMζ level in the nerve-injured group was significantly increased (*$P < 0.05$, Figure 9A) on POD 7 relative to the sham-injured group. Moreover, the expression level of p-PKMζ was significantly increased by nerve injury on POD 7 (Figure 9B, *$P < 0.05$).

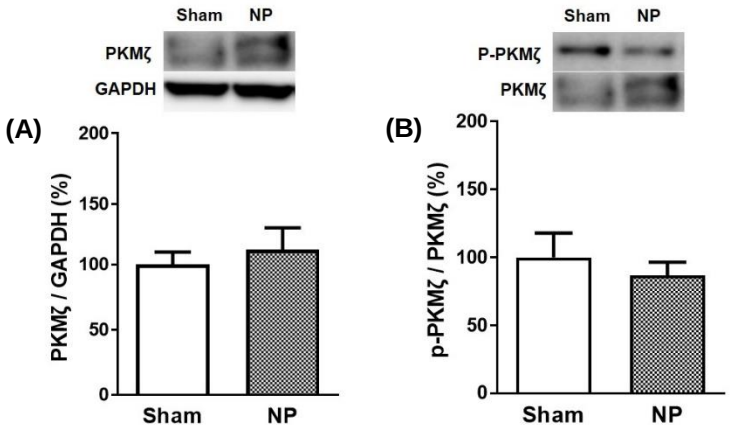


**Figure 8. Expression levels of PKMζ and p-PKMζ after nerve injury on POD 3.** (A) Expression levels of PKMζ normalized to GAPDH levels. There was no significant difference in PKMζ levels between the sham (n=6) and neuropathic pain (NP) groups (n=6, $P > 0.05$). (B) Expression levels of p-PKMζ normalized to PKMζ levels. After nerve injury on POD 3, there was no significant difference in p-PKMζ levels between the sham (n=6) and NP groups (n=6, $P > 0.05$).

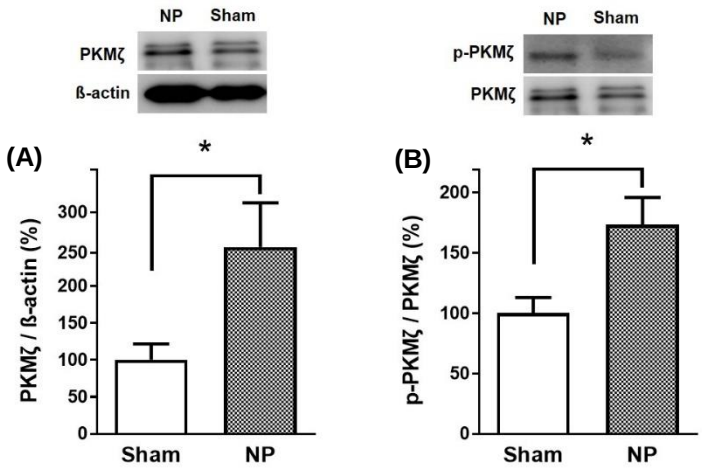


**Figure 9. Expression levels of PKMζ and p-PKMζ after nerve injury on POD 7.**
(A) Expression levels of PKMζ normalized to β-actin levels. After nerve injury (n=5) on POD 7, levels of PKMζ were significantly increased compared to sham group (n=5, *P < 0.05). (B) Expression levels of p-PKMζ normalized to PKMζ levels. After nerve injury on POD 7, levels of p-PKMζ were significantly increased between the sham (n=5) and NP groups (n=5, *P < 0.05).

E. GluR1 and GluR2 expression level after nerve injury

It would be important to know the level of GluR1 and GluR2 protein in IC before and after inducing neuropathic pain model in rat. Thus, GluR1 and GluR2 protein level were examined by western blotting after nerve injury. The GluR1 level in the nerve-injured group was not changed (Figure 10A, $P > 0.05$) on POD 3 relative to the sham-injured group. Moreover, the expression level of GluR2 was not changed by nerve injury on POD 3 (Figure 10B, $P > 0.05$). The GluR1 level in the nerve-injured group was not changed (Figure 11A, $P > 0.05$) on POD 7 relative to the sham-injured group. However, the expression level of GluR2 was significantly changed by nerve injury on POD 7 (Figure 11B, $*P < 0.05$).

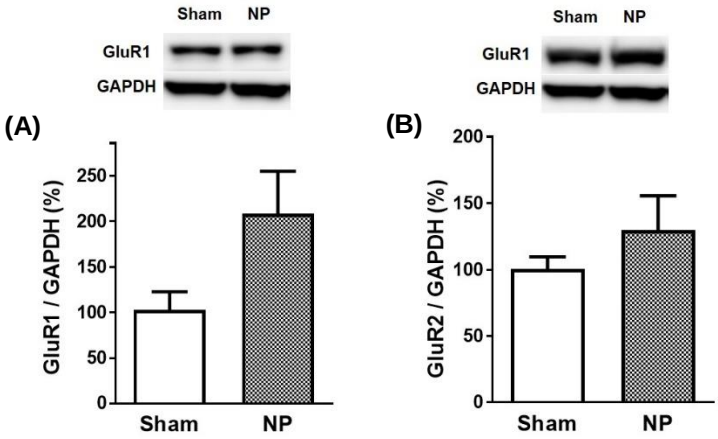


**Figure 10. Expression levels of GluR1 and GluR2 after nerve injury on POD 3.** (A) Expression levels of GluR1 normalized to GAPDH levels. There was no significant difference in GluR1 levels between the sham (n=6) and NP groups (n=6, $P > 0.05$). (B) Expression levels of GluR2 normalized to GAPDH levels. After nerve injury on POD 3, there was no significant difference in GluR2 levels between the sham (n=6) and neuropathic pain groups (n=6, $P > 0.05$).

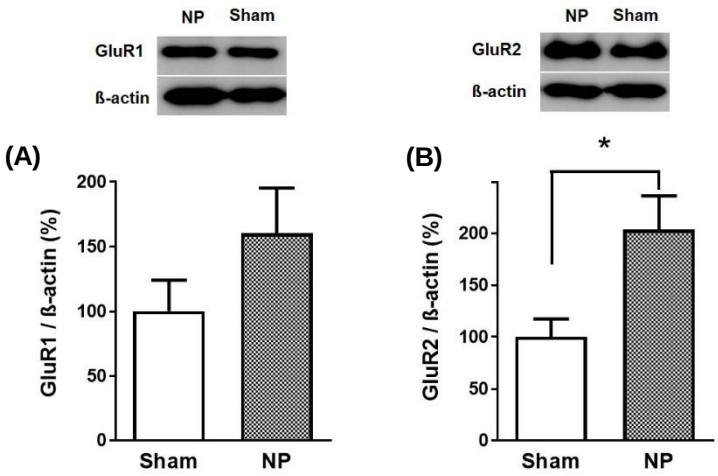


**Figure 11. Expression levels of GluR1 and GluR2 after nerve injury on POD 7.** (A) Expression levels of GluR1 normalized to β-actin levels. There was no significant difference in GluR1 levels between the sham (n=5) and NP groups (n=5, $P > 0.05$). (B) Expression levels of GluR2 normalized to β-actin levels. After nerve injury on POD 7, there were significantly increased GluR2 levels between the sham (n=5) and NP groups (n=5, $*P < 0.05$).

## IV. STUDY 3 : Modulation of the neuropathic pain by inhibition of PKMζ

### 1. Purpose of the study

In rodents, lesions of the IC can reverse neuropathic pain states to normal states, but do not affect non-nociceptive mechanical thresholds.[25,26] Jasmin et al.[13,15] showed that the IC has a key role in pain information processing and pain modulation.

ZIP, inhibitor of PKMζ, can reverse LTP maintenance and block the L-LTP formation.[47,48] For example, ZIP can also erase spatial, fear, addiction, and CTA memory involved in various CNS regions.[43,48-51] Moreover, several studies reported that PKMζ-related pain memory can be erased by ZIP in the spinal cord and brain.[8,52,53]

Therefore, to reveal the effect of the ZIP on pain modulation related to PKMζ of the IC the expression level of PKMζ, phosphor-PKMζ and analgesic effect after ZIP injection into the IC were confirmed. Thus, the purpose of study 3 is to investigate the role of the IC in pain modulation in relation to signaling pathways of PKMζ.

## 2. Materials and methods

### A. Animals

All experimental procedures in this study were conducted in accordance with the National Institute of Health guidelines and were approved by the Institutional Animal Care and Use Committee of the Yonsei University Health System. Male Sprague-Dawley rats (Koatec, Pyeongtaek, Korea, 130-150 g) were allowed to acclimate for a period of 7 days after arrival and were accommodated in the temperature-controlled room with food pellets and water provided ad libitum.

### B. Cannulation and neuropathic surgery

For cannula implantation, rats were anesthetized with sodium pentobarbital (50 mg/kg, i.p). 28-gauge guide cannulas were bilaterally implanted into the IC (AP: +1.0 mm, ML: ±4.7 mm, DV: -5.8 mm) on a stereotaxic frame. Rats were allowed to recover for 7 days after cannula implantation. Cannula-implanted rats were anesthetized with sodium pentobarbital (50 mg/kg, i.p.) and branches of the left sciatic nerve were exposed. The tibial and sural nerves were tightly ligated with 4-0 black silk and cut, while the common peroneal nerve was left intact.[54] The same procedure was applied to the sham-operated group without nerve injury. The wound was sutured in the muscle and skin layers.

### C. ZIP microinjection into the insular cortex, and analgesia test

ZIP microinjection was conducted on POD 3. A Hamilton syringe and PE-10 tubing were used with an injection cannula for microinjection. Saline or 10 nmol/μl of ZIP

(Tocris Bioscience, Minneapolis, MN, USA) diluted in saline (0.9% NaCl) was infused into the IC bilaterally, 0.5 μl per side. After injection, the injection canulas were maintained in position as they were for at least 1 min. The behavioral test was performed before ZIP injection, and 30 mins, 1, 2, 4, 8, 12, 24, and 48 hrs after microinjection.

D. Western blotting

To collect insular cortices, animals were anesthetized with enflurane and decapitated. The ipsilateral and contralateral rostral insular cortices were quickly isolated and transferred into a deep freezer. Extracted samples were stored at -70°C. For protein extraction, samples were homogenized by sonication in lysis buffer (Proprep, iNtRON Biotechnology Inc, Seongnam, Korea) containing phosphatase inhibitor (PhosStop, Roche, Penzberg, Germany). Samples were centrifuged at 22,250 g for 10 mins at 4°C and supernatants were collected, and total protein concentrations of lysates were assessed with a spectrophotometer (ND-1000, NanoDrop Technologies Inc, Wilmington, DE, USA). 10 μl of protein of brain tissue extracts was denatured per well and run on 10% Bis-Tris gels (Bio-Rad, Hercules, CA, USA) for detection of PKMζ, p-PKMζ, GluR1, and GluR2. Proteins were transferred onto polyvinylidene difluoride (PVDF) membranes (GE Healthcare, Buckinghamshire, UK). Membranes were blocked in 5% skim milk in TBS with Tween-20 for 1 hr and incubated in primary antibodies overnight on a rocking platform at 4°C. Primary antibodies against PKMζ (1:2,000, Cell Signaling Technology, Beverly, MA, USA), p-PKMζ (1:2,000, Cell Signaling Technology), GluR1 (1:2,000, Millipore, Temecula, MA, USA), GluR2 (1:2,000, Abcam), GAPDH (1:10,000, Ab Frontier, Seoul, Korea) and β-actin (1:10,000, Cell Signaling Technology) were used for western blotting. On the following day, the membranes were incubated in the appropriate secondary antibodies for 2 hrs and horseradish peroxidase activity was visualized using a

chemiluminescent substrate (ECL™ Prime western blotting detection reagent, GE Healthcare) and processed with a local allocation system (LAS) system (ImageQuant LAS 4000 Mini, GE Healthcare). The intensity of the bands for PKMζ, GluR1 and GluR2 were normalized to the intensity of GAPDH or β-actin. The intensity of the bands for p-PKMζ was normalized to the intensity of PKMζ.

E. Statistical analysis

Unpaired t-test for post-hoc comparison was used for two-group comparisons while two-way ANOVA with repeated measures was used to analyze behavioral test. Western blots and IHC were compared using an unpaired t-test. All data were expressed as the mean ± SEM. A p-value less than 0.05 was considered statistically significant.

## 3. Results

A. ZIP injection into the insular cortex

Figure 12A shows the injection site of the IC. Injection of ZIP into the IC decreased mechanical allodynia gradually on POD 3. The time course of mechanical allodynia in the ZIP-injected group on POD 3 shows that the analgesic effects of ZIP last for 12 hrs after injection (Figure 12B, *$P < 0.05$), where analgesia was measured relative to the saline-injected group. However, at 24 and 48 hrs after injection, ZIP had no significant effect ($P > 0.05$). The time course of mechanical allodynia in the ZIP-injected group on POD 7 shows that the analgesic effects of ZIP last for 12 hrs after injection (Figure 12C, *$P < 0.05$), where analgesia was measured relative to the saline-injected group. However, at 24 and 48 hrs after injection, ZIP had no significant pain relieving effect ($P > 0.05$).

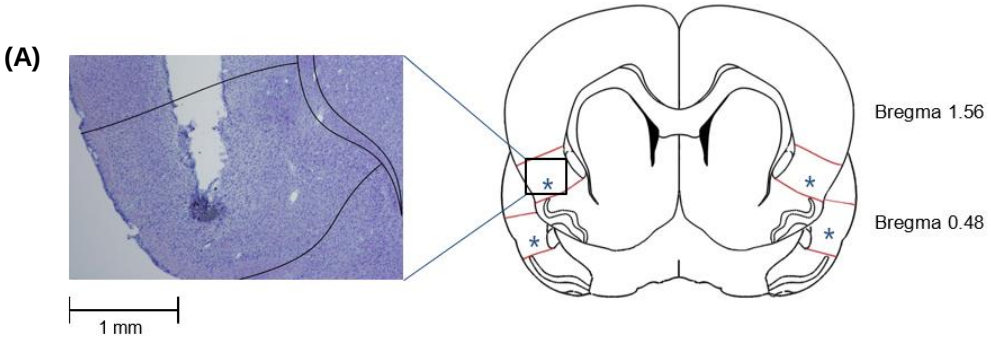


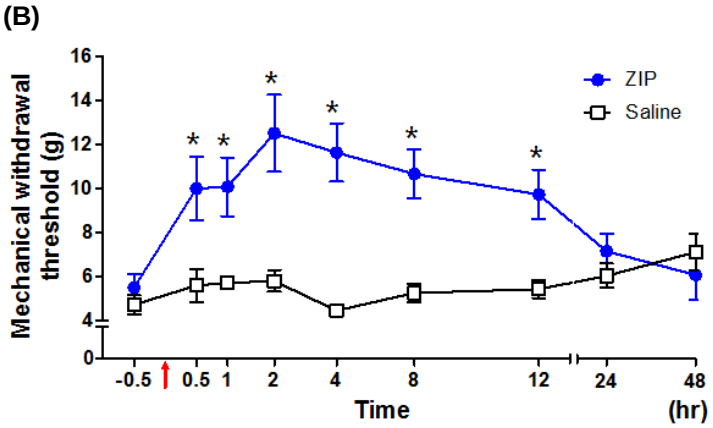


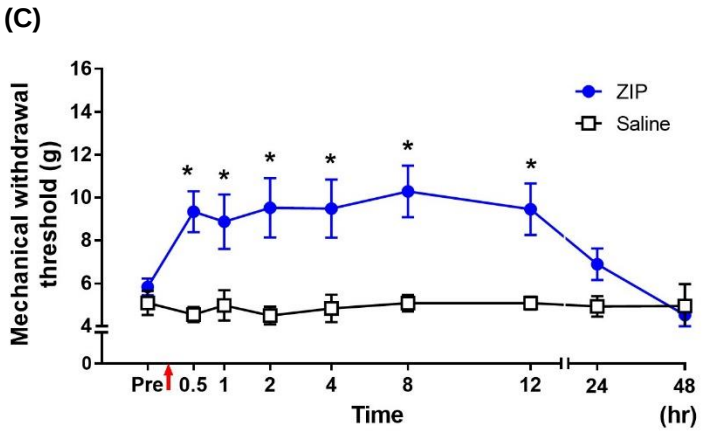

**Figure 12. Reduction of mechanical allodynia after ZIP microinjection into the IC.** (A) Identification of the ZIP injection site. ZIP was microinjected into the IC. (B) Paw withdrawal threshold to mechanical stimulation in POD 3 rats after microinjection of ZIP. Significant differences between ZIP-injected group (n=7) and saline-injected group (n=5) were found at the time points from 30 mins to 12 hrs after injection (two-way ANOVA repeated measures $P < 0.01$, unpaired t-test *$P < 0.05$). The arrow indicates the time point of ZIP or saline injection. (C) Paw withdrawal threshold to mechanical stimulation in POD 7 rats after microinjection of ZIP. Significant differences between ZIP-injected group (n=10) and saline-injected group (n=6) were found at the time points from 30 mins to 12 hrs after injection (two-way ANOVA repeated measures $P < 0.01$, unpaired t-test *$P < 0.05$).

B. Effects on PKMζ and p-PKMζ expression of ZIP microinjection into the insular cortex

To determine the role of ZIP, the IC was punched 3 hrs after ZIP injection. The total PKMζ in the ZIP-injected group was not changed (Figure 13A, $P > 0.05$) on POD 3 relative to the saline-injected group. However, the expression level of p-PKMζ was down-regulated by ZIP injection into the IC on POD 3 (Figure 13B, $*P < 0.05$). The results showed decreased PKMζ and p-PKMζ levels (Figures 14A and 14B, $*P < 0.05$) in the ZIP-injected group, relative to the saline-injected group on POD 7.

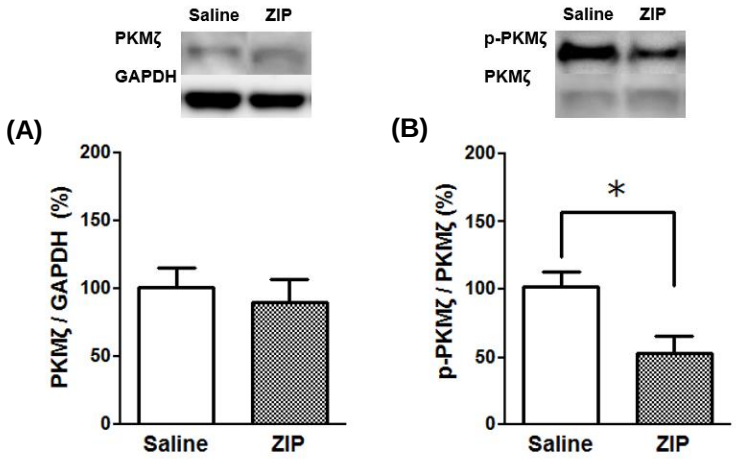


**Figure 13. Expression levels of PKMζ and p-PKMζ after ZIP microinjection into the IC on POD 3.** (A) Expression levels of PKMζ normalized to GAPDH levels. There was no significant difference in PKMζ levels between the saline-injected (n=6) and ZIP-injected groups (n=6, $P > 0.05$). (B) Expression levels of p-PKMζ normalized to PKMζ levels. After ZIP injection (n=6), p-PKMζ levels were significantly decreased (n=6, $*P < 0.05$).

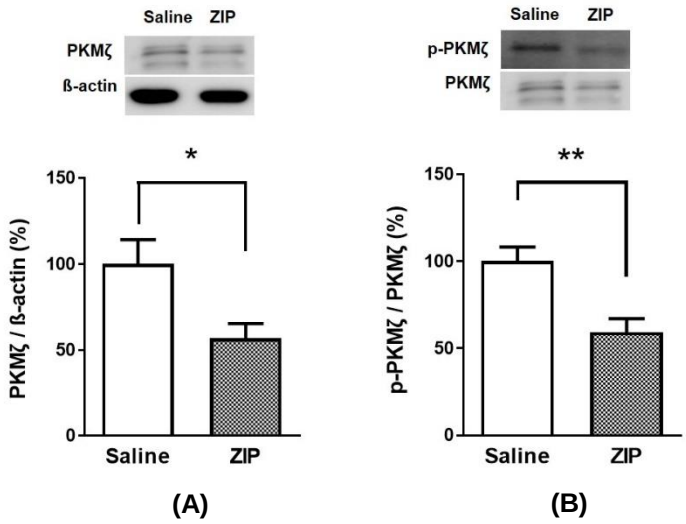


**Figure 14. Expression levels of PKMζ and p-PKMζ after ZIP microinjection into the IC on POD 7.** (A) Expression levels of PKMζ normalized to β-actin levels. There was significant difference in PKMζ levels between the saline-injected (n=5) and ZIP-injected groups (n=5, *P < 0.05). (B) Expression levels of p-PKMζ normalized to PKMζ levels. After ZIP injection (n=5), p-PKMζ levels were significantly decreased compared to saline-injected group (n=5, **P < 0.01).

C. Effects of ZIP microinjection into the insular cortex on GluR1 and GluR2 levels

It is speculated that the effects of ZIP may contribute to inhibition of AMPA receptors. Accordingly, the expression levels of the AMPA receptor subunits GluR1 and GluR2 were measured after ZIP microinjection on PODs 3 and 7. The results showed decreased GluR1 and GluR2 levels (Figures 15A and 15B, *P < 0.05) in the ZIP-injected group, relative to the saline-injected group on POD 3. The results showed decreased GluR2 levels (Figure 16B, *P < 0.05) in the ZIP-injected group, relative to the saline-injected group on POD 7.

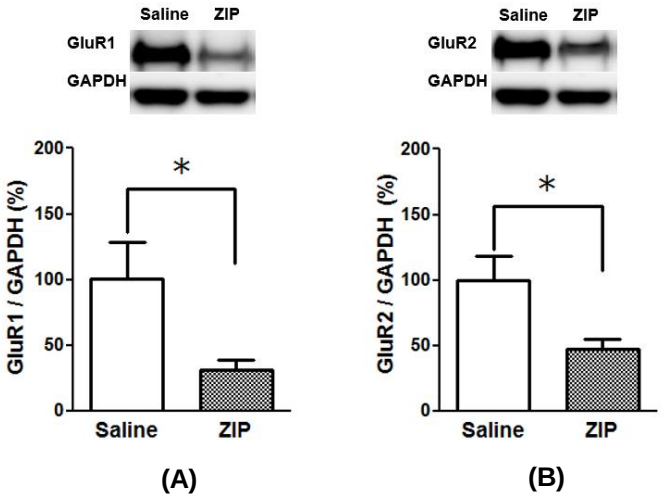


**Figure 15. Expression levels of GluR1 and GluR2 after ZIP microinjection into the IC on POD 3.** (A) Expression levels of GluR1 normalized to GAPDH levels. There was a significant difference between GluR1 levels in the saline-injected group (n=6) and ZIP-injected group (n=6, *P < 0.05). (B) Expression levels of GluR2 normalized to GAPDH levels. After ZIP injection (n=6), GluR2 levels were significantly decreased compared to saline-injected group (n=6, *P < 0.05).

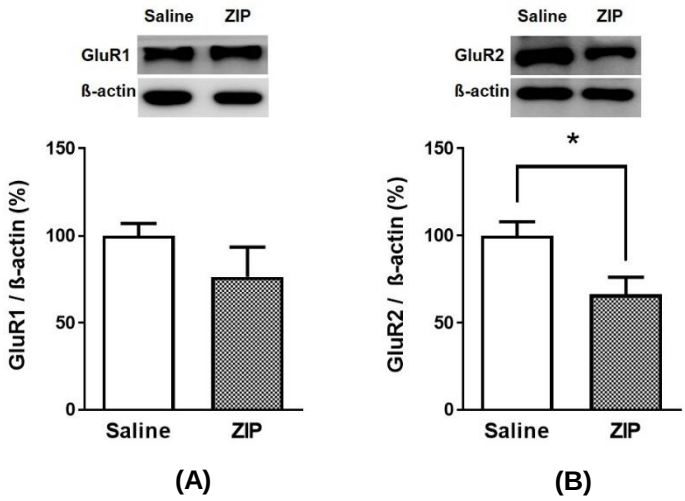


**Figure 16. Expression levels of GluR1 and GluR2 after ZIP microinjection into the IC on POD 7.** (A) Expression levels of GluR1 normalized to β-actin levels. There was no significant difference between GluR1 levels in the saline injection (n=5) and ZIP-injected group (n=5, $P > 0.05$). (B) Expression levels of GluR2 normalized to β-actin levels. After ZIP injection (n=5), GluR2 levels were significantly decreased compared to saline-injected group (n=5, $*P < 0.05$).

## V. DISCUSSION

The IC plays a role in interpretation of emotional aspects of pain as one of the limbic system areas.[16] Several studies have reported that plastic changes in the IC are induced by peripheral nerve injury.[44,59] Therefore, this study focused on plastic changes of the IC and its pain modulation after nerve injury in order to understand the mechanisms of chronic pain. Recent reports have shown that functional changes in the brain following nerve injury may be mainly mediated by LTP.[1,8] PKMζ, continuous active kinase, plays a key role in maintaining LTP, and inhibition of PKMζ can erase established memories and reverse the chronic pain state.[41,50] The purpose of this study is to determine whether the IC is a site of pain information processing, and if it exhibits plasticity after nerve injury. This is the first study to demonstrate optical signals in the IC induced by peripheral electrical stimulation in a neuropathic pain model. Specifically, optical signals were observed in the IC using VSD in response to electrical stimulation of the contralateral hind paw. Amplitudes and activated areas of optical signals in the IC were increased as the intensity of electrical stimulation was elevated. In addition, modification of excitability was observed in the IC after nerve injury. Together, these results shed light on the pain processing function of the IC in chronic pain states related to nerve injury-induced plastic changes.

A large number of neuroimaging studies have reported that noxious stimuli evoke activation of specific brain areas comprising the so called pain matrix.[6] Activation of the S1 and S2 is consistently observed in response to nociceptive stimulation in fMRI, PET, EEG, and MEG studies.[7,60,61] These areas have specialized subfunctions and handle the sensory-discriminative aspects of pain processing. On the other hand, emotional aspects of pain are represented in the limbic areas such as the ACC and IC.[1,12] In fact, the human S2 and posterior IC respond differently to $CO_2$ laser stimulation as determined by

electrode recording.[19] Specifically, whereas the S2 is sensitive to changes in the intensity of sub-threshold pain stimuli, the IC is sensitive to change in the level of painful stimuli.[19] According to an animal study, the S2 and IC are activated by hind paw electrical stimulation.[25] Consistent with this observation, the results in this study show that S2 and IC were activated by peripheral electrical stimulation. Interestingly, while the S2 was activated by stimuli ranging in intensity from low to high, the IC was only activated by high stimulation intensity. A high-resolution fMRI study demonstrated that the IC responds to painful infrared laser mechanical stimulation.[62] In addition, Craig et al.[63] used PET to observe cooling stimuli-evoked contralateral activation of the IC. Taken together, these reports suggest that the IC may be specifically activated by painful stimuli. In addition, data of in this study provide the first evidence that the IC can be activated by electrical stimulation in a neuropathic model using in vivo optical imaging. Given the number of pain-related studies based on fMRI studies and recent critiques doubtful of their validity due to an error in fMRI software,[64] the results of the present study are useful for confirming previous reports that the IC is indeed part of the pain matrix area.

The IC is located deep inside the lateral fissure in humans and, in addition to gustatory functions, plays a critical role in the interpretation of the emotional aspects of pain.[16] Jasmin et al.[13,15] showed that the IC has efferent and afferent connections to nociceptive processing areas and can change the pain threshold using GABA neurotransmission. However, there have been relatively few studies regarding excitability in the IC in chronic pain models. In the present study, it was found that optical signals of the IC were increased in the neuropathic and sham group as peripheral stimulation increased. On the other hand, the neuropathic group showed high optical signals in response to low stimulation while the sham group showed low optical signals in response to high intensity stimulation, which was consistent with the human imaging studies described above.[23,24]

In this study, optical intensities and activated areas seem to be related to neuronal activation in response to pain sensation. To date, there was no optical imaging study observing changes in the IC. However, it can be found that the meaning of increases in optical intensity and activated area in electrophysiological and imaging studies. For example, scores on visual-analogue scale increase and laser-evoked potentials increase as intensities in peripheral stimulation increase.[19] In this case, laser-evoked potentials can correspond to optical intensity. Another study reported that as the pain sensation becomes more intense, the more laser-evoked potentials in the operculoinsular and primary somatosensory areas are observed.[22] An fMRI study using heat/capsaicin sensitization model showed that the more activated areas were observed in humans with hyperalgesia compared to controls.[65] An animal study using fMRI reported that BOLD signals and activated areas increased in brain areas including the IC in hyperalgesia rats.[66]

In the present study, different intensities of peripheral stimulation showed the differences in optical signals including both peak intensities and activated areas between neuropathic and sham-operated rats. The peak amplitude evoked by 5.0 mA electrical stimulation of nerve-injured rats was increased compared to sham-operated rats. The activated area evoked by 1.25 and 2.5 mA electrical stimulation in nerve-injured rats was increased compared to sham-operated rats. However, there was no significant difference in activated areas between nerve-injured and sham groups following 5.0 mA stimulation. Therefore, there may be some discrepancies between peak amplitudes and activated areas in this results. It is can be difficult to explain these discrepancies in detail solely by this study. But it was speculate that the activated area in neuropathic rats is likely to become saturated readily at relatively low stimulation intensities and the activated area in sham controls approaches the saturation level at intense stimulation (5.0 mA) because the region of interest (ROI) is relatively small area in the IC. In contrast, it seems that the

peak amplitude is not saturated readily and shows more sensitive responses to increasing stimulation intensities in neuropathic rats.

There are a variety of plastic changes in pain-related brain areas in the chronic pain state. Patients with chronic back pain due to neuropathic and non-neuropathic causes have decreased gray matter density in the central nervous system.[67,68] According to several animal studies, functional and structural plastic changes in the S1, S2, and PFC have been reported.[69] The ACC is considered to be related to the emotional aspects of pain as part of the limbic system.[1] Recently, Li et al.[8] demonstrated that nerve injury-induced plasticity in the ACC contributes to chronic pain, and that elimination of this plasticity can reverse the chronic pain state. In addition to the ACC, several studies have observed that peripheral nerve injury induces functional plasticity in the IC related to NMDA and AMPA receptors.[44,59] Taken together, these results suggest that plasticity of the IC induced by nerve injury may contribute to chronification of neuropathic pain. In line with these reports, it was observed in the present study that the amplitudes and activated areas of optical signals to the peripheral stimulation were significantly increased in the neuropathic pain group compared to the control group. It was speculated that this phenomenon was due to nerve injury-induced plasticity in the IC. However, as there are few reports about nerve injury-induced plasticity of the IC and its contribution to chronic pain, it will be necessary to explore the IC in greater detail in future studies.

Zif268 is a well-known marker related to LTP and neuronal plasticity.[45] In the hippocampus, the L-LTP phase requires the expression of IEGs such as zif268 and activity-regulated cytoskeletal-associated protein.[70,71] LTP-inducing stimulation increases zif268 expression levels in the hippocampus.[72] Furthermore, zif268 knockout mice displayed an absence of L-LTP and impaired long-term memory.[45] c-Fos is a neuronal activation marker and is expressed highly after nerve injury in the spinal cord and ACC.[8]

Expression of c-Fos in the IC is increased by stress-induced hyperalgesia.[73] However, since zif268 is more correlated with LTP and plasticity to a greater degree than is c-Fos,[74] changes in zif268 expression level in the IC after nerve injury were assessed immunohistochemically in this study. There have been several reports that zif268 is induced by nociceptive stimulation.[74,75] However, there have been no reports on zif268 expression related to nerve injury-induced plasticity in the IC. The results show that the number of zif268-positive cells increased after nerve injury, which is related to nerve injury-induced LTP in the IC.

Findings of this study suggest that PKMζ in the IC can lead to nerve injury-induced plasticity which contributes to the maintenance of neuropathic pain states. PKMζ is a key molecule for maintaining L-LTP and inhibition of PKMζ can erase established LTP.[41,50] Although the functions of PKMζ were controversial by some studies,[76-78] recent studies have suggested that atypical PKCs compensate the role of PKMζ in maintaining LTP in the constitutive PKMζ knock-out mice.[79] In fact, many studies have reported that the administration of ZIP into the spinal cord can reverse inflammatory pain, but not neuropathic pain.[52,53,80,81] In contrast, ZIP injection into the ACC reverses the neuropathic pain state, but the analgesic effects disappear 24 hrs after injection of ZIP.[8] Because the concentration of 10 nmol/μl ZIP effectively impaired learning[43,48] or reversed pain threshold,[8] concentration of ZIP was 10 nmol/μl in this study. Based on these report, the effects of ZIP injection into the IC were investigated in the present study. The effects of ZIP lasted for 12 hrs after injection into the IC, but the pain-relieving effect was not permanent. This may be due to the reestablishment of LTP by the tonic peripheral afferent drive.[8,81]

PKMζ was selectively upregulated in the spinal cord by formalin, capsaicin, and nerve injury.[53,81] In the ACC, both PKMζ and p-PKMζ increased after nerve injury.[8] PKMζ is

activated by phosphorylation and can be inhibited by ZIP.[50] Increased levels of p-PKMζ in the ACC contribute to neuropathic pain.[8] Similarly, increased levels of p-PKMζ in the spinal cord contribute to formalin-induced pain.[80] Taken together, it was hypothesized that upregulation of p-PKMζ in the IC might contribute to neuropathic pain states and ZIP can alleviate neuropathic pain. Indeed, decreased levels of p-PKMζ were observed following ZIP injection in this study. In contrast, intrathecal infusion of ZIP did not reduce p-PKMζ levels in the spinal cords of formalin model rats.[80] Although the results are inconsistent with these studies, the results show that the function of p-PKMζ in the IC differs from that in the spinal cord, and these results are in line with those found with respect to the ACC.[8]

Several reports have suggested that trafficking of the GluR2 subunit of the AMPA receptor in the hippocampus is related to PKMζ.[41,82] In addition, fear memory is maintained by PKMζ-mediated GluR2-dependent AMPA receptor trafficking in the amygdala.[83] Other reports suggest that the GluR1 subunit of the AMPA receptor is involved in the molecular machinery of cocaine-induced plasticity in the nucleus accumbens (NAc).[84,85] PKMζ-mediated LTP expression may be induced by N-ethylmaleimide-sensitive factor/GluR2-dependent trafficking in the hippocampus.[82] Interestingly, the results show that both GluR1 and GluR2 levels are down-regulated by ZIP injection in the neuropathic pain model rats. Consistent with this, GluR1 levels were decreased after ZIP injection into the ACC of neuropathic pain model.[8] Other report suggests that activation of mGluR1 is required for insular L-LTP induction.[86] In addition, administration of ZIP into the NAc core can abolish long-term drug reward memory by effect on GluR2-containing AMPA receptors.[87] Taken together, it was assumed that PKMζ maintains pain-related long-term plastic changes in the IC via both the GluR1 and GluR2 subunits of AMPA receptors.

## VI. CONCLUSIONS

Because optical imaging using VSD has a high spatial and temporal resolution, this technique is suitable to detect direct responses of the IC. Using an optical imaging technique, it is demonstrated that two major changes in peak amplitude and activated area in the IC elicited by peripheral electrical stimulation after nerve injury. The result also demonstrated the presence of nerve injury-induced plasticity in the IC, and suggested that the IC can be a target of chronic pain modulation.

This study demonstrated that there is a correlation between PKMζ and neural plasticity of the IC, which might explain chronic pain mechanisms. PKMζ seems to mediate this plasticity by regulating AMPA receptors containing GluR1 and GluR2. Moreover, the pain modulation function of the IC related to PKMζ was revealed through administration of ZIP. Pharmacological targeting to inhibit plasticity of the IC may therefore present a strategy for chronic neuropathic pain therapy.

Further studies on the detailed characteristics of plasticity in the IC will be necessary to elucidate the specific mechanisms of nerve injury-induced plastic changes in the IC.

## REFERENCES

1. Zhuo M. Cortical excitation and chronic pain. Trends Neurosci 2008;31:199-207.
2. Reichling DB, Levine JD. Critical role of nociceptor plasticity in chronic pain. Trends Neurosci 2009;32:611-8.
3. Ruscheweyh R, Wilder-Smith O, Drdla R, Liu XG, Sandkuhler J. Long-term potentiation in spinal nociceptive pathways as a novel target for pain therapy. Mol Pain 2011;7:20.
4. Woolf CJ, Salter MW. Neuronal plasticity: increasing the gain in pain. Science 2000;288:1765-9.
5. Melzack R. From the gate to the neuromatrix. Pain 1999;Suppl 6:S121-6.
6. Iannetti GD, Mouraux A. From the neuromatrix to the pain matrix (and back). Exp Brain Res 2010;205:1-12.
7. Apkarian AV, Bushnell MC, Treede RD, Zubieta JK. Human brain mechanisms of pain perception and regulation in health and disease. Eur J Pain 2005;9:463-84.
8. Li XY, Ko HG, Chen T, Descalzi G, Koga K, Wang H, et al. Alleviating neuropathic pain hypersensitivity by inhibiting PKMzeta in the anterior cingulate cortex. Science 2010;330:1400-4.
9. Xu H, Wu LJ, Wang H, Zhang X, Vadakkan KI, Kim SS, et al. Presynaptic and postsynaptic amplifications of neuropathic pain in the anterior cingulate cortex. J Neurosci 2008;28:7445-53.
10. Kim SK, Nabekura J. Rapid synaptic remodeling in the adult somatosensory cortex following peripheral nerve injury and its association with neuropathic pain. J Neurosci 2011;31:5477-82.
11. Metz AE, Yau HJ, Centeno MV, Apkarian AV, Martina M. Morphological and functional reorganization of rat medial prefrontal cortex in neuropathic pain. Proc Natl Acad Sci U S A 2009;106:2423-8.
12. Craig AD. How do you feel? Interoception: the sense of the physiological condition of the body. Nat Rev Neurosci 2002;3:655-66.

13. Jasmin L, Rabkin SD, Granato A, Boudah A, Ohara PT. Analgesia and hyperalgesia from GABA-mediated modulation of the cerebral cortex. Nature 2003;424:316-20.
14. Lu CB, Yang T, Zhao H, Zhang M, Meng FC, Fu H, et al. Insular cortex is critical for the perception, modulation, and chronification of pain. Neurosci Bull 2016;32:191-201.
15. Jasmin L, Burkey AR, Granato A, Ohara PT. Rostral agranular insular cortex and pain areas of the central nervous system: a tract-tracing study in the rat. J Comp Neurol 2004;468:425-40.
16. Craig AD. Interoception: the sense of the physiological condition of the body. Curr Opin Neurobiol 2003;13:500-5.
17. Alvarez P, Dieb W, Hafidi A, Voisin DL, Dallel R. Insular cortex representation of dynamic mechanical allodynia in trigeminal neuropathic rats. Neurobiol Dis 2009;33:89-95.
18. Berthier M, Starkstein S, Leiguarda R. Asymbolia for pain: a sensory-limbic disconnection syndrome. Ann Neurol 1988;24:41-9.
19. Frot M, Magnin M, Mauguiere F, Garcia-Larrea L. Human SII and posterior insula differently encode thermal laser stimuli. Cereb Cortex 2007;17:610-20.
20. Mazzola L, Isnard J, Peyron R, Guenot M, Mauguiere F. Somatotopic organization of pain responses to direct electrical stimulation of the human insular cortex. Pain 2009;146:99-104.
21. Ostrowsky K, Magnin M, Ryvlin P, Isnard J, Guenot M, Mauguiere F. Representation of pain and somatic sensation in the human insula: a study of responses to direct electrical cortical stimulation. Cerebral Cortex 2002;12:376-85.
22. Iannetti GD, Zambreanu L, Cruccuc G, Tracey I. Operculoinsular cortex encodes pain intensity at the earliest stages of cortical processing as indicated by amplitude of laser-evoked potentials in humans. Neuroscience 2005;131:199-208.
23. Morgan V, Pickens D, Gautam S, Kessler R, Mertz H. Amitriptyline reduces rectal pain related activation of the anterior cingulate cortex in patients with irritable bowel syndrome. Gut 2005;54:601-7.

24. Stern J, Jeanmonod D, Sarnthein J. Persistent EEG overactivation in the cortical pain matrix of neurogenic pain patients. Neuroimage 2006;31:721-31.

25. Benison AM, Chumachenko S, Harrison JA, Maier SF, Falci SP, Watkins LR, et al. Caudal granular insular cortex is sufficient and necessary for the long-term maintenance of allodynic behavior in the rat attributable to mononeuropathy. J Neurosci 2011;31:6317-28.

26. Coffeen U, Manuel Ortega-Legaspi J, Lopez-Munoz FJ, Simon-Arceo K, Jaimes O, Pellicer F. Insular cortex lesion diminishes neuropathic and inflammatory pain-like behaviours. Eur J Pain 2011;15:132-8.

27. Grinvald A, Hildesheim R. VSDI: a new era in functional imaging of cortical dynamics. Nat Rev Neurosci 2004;5:874-85.

28. An S, Yang JW, Sun H, Kilb W, Luhmann HJ. Long-term potentiation in the neonatal rat barrel cortex in vivo. J Neurosci 2012;32:9511-6.

29. Chae Y, Park HJ, Hahm DH, Lee BH, Park HK, Lee H. Spatiotemporal patterns of neural activity in response to electroacupuncture stimulation in the rodent primary somatosensory cortex. Neurol Res 2010;32 Suppl 1:64-8.

30. Fehervari TD, Okazaki Y, Sawai H, Yagi T. In vivo voltage-sensitive dye study of lateral spreading of cortical activity in mouse primary visual cortex induced by a current impulse. PLoS One 2015;10:e0133853.

31. Kobayashi M, Fujita S, Takei H, Song L, Chen S, Suzuki I, et al. Functional mapping of gustatory neurons in the insular cortex revealed by pERK-immunohistochemistry and in vivo optical imaging. Synapse 2010;64:323-34.

32. Noto M, Nishikawa J, Tateno T. An analysis of nonlinear dynamics underlying neural activity related to auditory induction in the rat auditory cortex. Neuroscience 2016;318:58-83.

33. Cha MH, Kim DS, Cho ZH, Sohn JH, Chung MA, Lee HJ, et al. Modification of cortical excitability in neuropathic rats: a voltage-sensitive dye study. Neurosci Lett 2009;464:117-21.

34. Suzuki R, Dickenson A. Spinal and supraspinal contributions to central sensitization in peripheral neuropathy. Neurosignals 2005;14:175-81.
35. Bliss TV, Collingridge GL. A synaptic model of memory: long-term potentiation in the hippocampus. Nature 1993;361:31-9.
36. Cooke SF, Bliss TV. Plasticity in the human central nervous system. Brain 2006;129:1659-73.
37. Sandkuhler J, Liu X. Induction of long-term potentiation at spinal synapses by noxious stimulation or nerve injury. Eur J Neurosci 1998;10:2476-80.
38. Ikeda H, Stark J, Fischer H, Wagner M, Drdla R, Jager T, et al. Synaptic amplifier of inflammatory pain in the spinal dorsal horn. Science 2006;312:1659-62.
39. Ji RR, Kohno T, Moore KA, Woolf CJ. Central sensitization and LTP: do pain and memory share similar mechanisms? Trends Neurosci 2003;26:696-705.
40. Ling DS, Benardo LS, Serrano PA, Blace N, Kelly MT, Crary JF, et al. Protein kinase Mzeta is necessary and sufficient for LTP maintenance. Nat Neurosci 2002;5:295-6.
41. Sacktor TC. PKMzeta, LTP maintenance, and the dynamic molecular biology of memory storage. Prog Brain Res 2008;169:27-40.
42. Sacktor TC, Osten P, Valsamis H, Jiang X, Naik MU, Sublette E. Persistent activation of the zeta isoform of protein kinase C in the maintenance of long-term potentiation. Proc Natl Acad Sci U S A 1993;90:8342-6.
43. Shema R, Sacktor TC, Dudai Y. Rapid erasure of long-term memory associations in the cortex by an inhibitor of PKM zeta. Science 2007;317:951-3.
44. Qiu S, Chen T, Koga K, Guo YY, Xu H, Song Q, et al. An increase in synaptic NMDA receptors in the insular cortex contributes to neuropathic pain. Sci Signal 2013;6:ra34.
45. Jones MW, Errington ML, French PJ, Fine A, Bliss TV, Garel S, et al. A requirement for the immediate early gene Zif268 in the expression of late LTP and long-term memories. Nat Neurosci 2001;4:289-96.

46. Haugan F, Wibrand K, Fiska A, Bramham CR, Tjolsen A. Stability of long term facilitation and expression of zif268 and Arc in the spinal cord dorsal horn is modulated by conditioning stimulation within the physiological frequency range of primary afferent fibers. Neuroscience 2008;154:1568-75.

47. Serrano P, Yao Y, Sacktor TC. Persistent phosphorylation by protein kinase Mzeta maintains late-phase long-term potentiation. J Neurosci 2005;25:1979-84.

48. Pastalkova E, Serrano P, Pinkhasova D, Wallace E, Fenton AA, Sacktor TC. Storage of spatial information by the maintenance mechanism of LTP. Science 2006;313:1141-4.

49. Serrano P, Friedman EL, Kenney J, Taubenfeld SM, Zimmerman JM, Hanna J, et al. PKMzeta maintains spatial, instrumental, and classically conditioned long-term memories. PLoS Biol 2008;6:2698-706.

50. Price TJ, Ghosh S. ZIPping to pain relief: the role (or not) of PKMzeta in chronic pain. Mol Pain 2013;9:6.

51. Velez-Hernandez ME, Vazquez-Torres R, Velasquez-Martinez MC, Jimenez L, Baez F, Sacktor TC, et al. Inhibition of protein kinase Mzeta (PKMzeta) in the mesolimbic system alters cocaine sensitization in rats. J Drug Alcohol Res 2013;2:235669.

52. Asiedu MN, Tillu DV, Melemedjian OK, Shy A, Sanoja R, Bodell B, et al. Spinal protein kinase M zeta underlies the maintenance mechanism of persistent nociceptive sensitization. J Neurosci 2011;31:6646-53.

53. Laferriere A, Pitcher MH, Haldane A, Huang Y, Cornea V, Kumar N, et al. PKMzeta is essential for spinal plasticity underlying the maintenance of persistent pain. Mol Pain 2011;7:99.

54. Lee BH, Won R, Baik EJ, Lee SH, Moon CH. An animal model of neuropathic pain employing injury to the sciatic nerve branches. Neuroreport 2000;11:657-61.

55. Lee KH, Kim UJ, Park YG, Won R, Lee H, Lee BH. Optical imaging of somatosensory evoked potentials in the rat cerebral cortex after spinal cord injury. J Neurotrauma 2011;28:797-807.

56. Saito M, Toyoda H, Kawakami S, Sato H, Bae YC, Kang Y. Capsaicin Induces Theta-Band Synchronization between Gustatory and Autonomic Insular Cortices. J Neurosci 2012;32:13470-87.

57. Fujita S, Adachi K, Koshikawa N, Kobayashi M. Spatiotemporal dynamics of excitation in Rat Insular Cortex: intrinsic corticocortical circuit regulates caudal-rostro excitatory propagation from the insular to frontal cortex. Neuroscience 2010;165:278-92.

58. Paxinos G, Watson C. The rat brain in stereotaxic coordinates. 6th ed. Amsterdam; Boston; Academic Press/Elsevier; 2007.

59. Qiu S, Zhang M, Liu Y, Guo Y, Zhao H, Song Q, et al. GluA1 phosphorylation contributes to postsynaptic amplification of neuropathic pain in the insular cortex. J Neurosci 2014;34:13505-15.

60. Garcia-Larrea L, Frot M, Valeriani M. Brain generators of laser-evoked potentials: from dipoles to functional significance. Neurophysiol Clin 2003;33:279-92.

61. Bushnell MC, Apkarian, A.V. Representation of pain in the brain. In: McMahon S, Koltzenburg M (eds) Textbook of pain, 5th edn. : Churchill Livingstone; 2005.

62. Baumgartner U, Iannetti GD, Zambreanu L, Stoeter P, Treede RD, Tracey I. Multiple somatotopic representations of heat and mechanical pain in the operculo-insular cortex: a high-resolution fMRI study. J Neurophysiol 2010;104:2863-72.

63. Craig AD, Chen K, Bandy D, Reiman EM. Thermosensory activation of insular cortex. Nat Neurosci 2000;3:184-90.

64. Eklund A, Nichols TE, Knutsson H. Cluster failure: Why fMRI inferences for spatial extent have inflated false-positive rates. Proc Natl Acad Sci U S A 2016;113:7900-5.

65. Zambreanu L, Wise RG, Brooks JC, Iannetti GD, Tracey I. A role for the brainstem in central sensitisation in humans. Evidence from functional magnetic resonance imaging. Pain 2005;114:397-407.

66. Hess A, Sergejeva M, Budinsky L, Zeilhofer HU, Brune K. Imaging of hyperalgesia in rats by functional MRI. Eur J Pain 2007;11:109-19.

67. Apkarian AV, Sosa Y, Sonty S, Levy RM, Harden RN, Parrish TB, et al. Chronic back pain is associated with decreased prefrontal and thalamic gray matter density. J Neurosci 2004;24:10410-5.

68. Schmidt-Wilcke T, Leinisch E, Ganssbauer S, Draganski B, Bogdahn U, Altmeppen J, et al. Affective components and intensity of pain correlate with structural differences in gray matter in chronic back pain patients. Pain 2006;125:89-97.

69. Kim W, Kim SK. Neural circuit remodeling and structural plasticity in the cortex during chronic pain. Korean J Physiol Pharmacol 2016;20:1-8.

70. Shepherd JD, Bear MF. New views of Arc, a master regulator of synaptic plasticity. Nat Neurosci 2011;14:279-84.

71. Granado N, Ortiz O, Suarez LM, Martin ED, Cena V, Solis JM, et al. D1 but not D5 dopamine receptors are critical for LTP, spatial learning, and LTP-Induced arc and zif268 expression in the hippocampus. Cereb Cortex 2008;18:1-12.

72. Ranieri F, Podda MV, Riccardi E, Frisullo G, Dileone M, Profice P, et al. Modulation of LTP at rat hippocampal CA3-CA1 synapses by direct current stimulation. J Neurophysiol 2012;107:1868-80.

73. Takeda R, Watanabe Y, Ikeda T, Abe H, Ebihara K, Matsuo H, et al. Analgesic effect of milnacipran is associated with c-Fos expression in the anterior cingulate cortex in the rat neuropathic pain model. Neurosci Res 2009;64:380-4.

74. Wisden W, Errington ML, Williams S, Dunnett SB, Waters C, Hitchcock D, et al. Differential expression of immediate early genes in the hippocampus and spinal cord. Neuron 1990;4:603-14.

75. Rygh LJ, Suzuki R, Rahman W, Wong Y, Vonsy JL, Sandhu H, et al. Local and descending circuits regulate long-term potentiation and zif268 expression in spinal neurons. Eur J Neurosci 2006;24:761-72.

76. Lee AM, Kanter BR, Wang D, Lim JP, Zou ME, Qiu C, et al. Prkcz null mice show normal learning and memory. Nature 2013;493:416-9.

77. Volk LJ, Bachman JL, Johnson R, Yu Y, Huganir RL. PKM-zeta is not required for hippocampal synaptic plasticity, learning and memory. Nature 2013;493:420-3.

78. Wu-Zhang AX, Schramm CL, Nabavi S, Malinow R, Newton AC. Cellular pharmacology of protein kinase Mzeta (PKMzeta) contrasts with its in vitro profile: implications for PKMzeta as a mediator of memory. J Biol Chem 2012;287:12879-85.

79. Tsokas P, Hsieh C, Yao Y, Lesburgueres E, Wallace EJ, Tcherepanov A, et al. Compensation for PKMzeta in long-term potentiation and spatial long-term memory in mutant mice. Elife 2016;5.

80. Marchand F, D'Mello R, Yip PK, Calvo M, Muller E, Pezet S, et al. Specific involvement of atypical PKCzeta/PKMzeta in spinal persistent nociceptive processing following peripheral inflammation in rat. Mol Pain 2011;7:86.

81. King T, Qu C, Okun A, Melemedjian OK, Mandell EK, Maskaykina IY, et al. Contribution of PKMzeta-dependent and independent amplification to components of experimental neuropathic pain. Pain 2012;153:1263-73.

82. Yao Y, Kelly MT, Sajikumar S, Serrano P, Tian D, Bergold PJ, et al. PKM zeta maintains late long-term potentiation by N-ethylmaleimide-sensitive factor/GluR2-dependent trafficking of postsynaptic AMPA receptors. J Neurosci 2008;28:7820-7.

83. Migues PV, Hardt O, Wu DC, Gamache K, Sacktor TC, Wang YT, et al. PKMzeta maintains memories by regulating GluR2-dependent AMPA receptor trafficking. Nat Neurosci 2010;13:630-4.

84. Shabashov D, Shohami E, Yaka R. Inactivation of PKMzeta in the NAc shell abolished cocaine-conditioned reward. J Mol Neurosci 2012;47:546-53.

85. Sutton MA, Schmidt EF, Choi KH, Schad CA, Whisler K, Simmons D, et al. Extinction-induced upregulation in AMPA receptors reduces cocaine-seeking behaviour. Nature 2003;421:70-5.

86. Liu MG, Kang SJ, Shi TY, Koga K, Zhang MM, Collingridge GL, et al. Long-term potentiation of synaptic transmission in the adult mouse insular cortex: multielectrode array recordings. J Neurophysiol 2013;110:505-21.

87. Li YQ, Xue YX, He YY, Li FQ, Xue LF, Xu CM, et al. Inhibition of PKMzeta in nucleus accumbens core abolishes long-term drug reward memory. J Neurosci 2011;31:5436-46.

**ABSTRACT (IN KOREAN)**

# 신경손상에 의해 유발된 insular cortex의 신경가소성이 신경병증성 통증에 미치는 영향

<지도교수 이 배 환>

연세대학교 대학원 의과학과

한 정 수

뇌섬엽 (insular cortex; IC)은 전통적으로 미각에 관여하는 것으로 알려져왔다. 최근의 보고들에 따르면, IC는 통증, 감정 및 신체의 항상성 조절과 관련된 다양한 기능을 수행 할 수 있다고 보고되고 있다. IC는 다양한 유형의 감각 입력을 받고 통증의 정서적인 측면을 처리하는 통증 관련 뇌 영역 중 하나로, 말초신경 손상은 IC의 신경가소성을 유발시킬 수 있으며 결과적으로 만성통증에 기여할 수 있다. 그러나, 신경 손상 후 IC의 신경가소성과 통증 조절의 관계에 대한 체계적인 연구는 현재까지 거의 없다. 따라서 본 연구는 말초 신경 손상 후 IC의 가소성 변화를 관찰하고, 이러한 신경가소성을 조절함으로써 통증완화효과를 관찰하기 위해 수행되었다.

첫 번째 세부연구는 전압 민감성 염료를 이용한 광영상을 통해 신경 손상 후 IC의 흥분성 변화와 관련된 활성화 패턴을 시공간적으로 조사하기 위해 수행되었다. Pentobarbital 마취 하에서 쥐의 경골신경과 비복신경을 손상시킨 뒤 손상 후 7 일 후에 IC에서 광학 신호를 관찰하기 위해 통증모델을 우레탄

으로 마취시키고 두개절제술을 시행했다. IC의 광 신호는 말초 전기 자극에 의해 유발되었다. 신경병증성통증 모델은 대조군에 비하여 5.0 mA 전기 자극에 의해 유의미하게 높은 광신호 강도를 보였다. 또한 대조군에 비하여 1.25 및 2.5 mA 전기 자극에 의해 더 넓은 광신호 활성 영역이 관찰되었다. 광신호가 활성화 된 영역은 자극강도가 강해질수록 더 넓어지는 경향이 있었으며, 광 신호의 최대 진폭은 자극 강도가 증가함에 따라 증가했다. 이러한 결과는 말초 자극에 대한 IC의 높은 흥분성이 신경병증성 통증과 관련이 있으며 신경손상 후 IC의 신경가소성이 발생하였을 가능성이 있음을 시사한다.

두 번째 세부연구는 신경 손상 후 IC의 단백질 인산화효소 Mζ (PKMζ) 관련 가소성을 관찰하기 위해 면역조직화학염색과 웨스턴 블로팅기법을 이용하여 수행되었다. 지속적으로 활성상태를 유지할 수 있는 인산화효소인 PKMζ는 기능적 신경가소성 중 한가지인 late-long term potentiation (L-LTP) 단계를 유지하는 것으로 알려져 있다. Zif268은 신경가소성과 LTP의 생체표지인자로 알려져 왔으며 PKMζ의 발현에도 관여한다고 알려진 분자이다. Zif268 면역조직화학염색은 신경손상 후 신경가소성이 IC에서 발생하는지, IC가 통증정보처리에 연관되어있는 영역인지 확인하기 위해 수행되었다. 기계적 이질통 검사와 zif268 면역조직화학염색은 신경 손상 후 수행되었다. 그 결과, IC에서 zif268 발현 량은 신경손상에 의해 의미 있게 증가하였다. 신경 손상 후 웨스턴 블로팅을 수행하여 L-LTP의 유지에 관여하는 PKMζ, phosphorylated PKMζ (p-PKMζ)의 발현을 측정 하였다. 그 결과, 신경손상 3일 후 신경손상 모델에서 PKMζ 및 p-PKMζ의 발현량은 대조군의 발현량에 비해 증가된 경향이 있었지만, 유의한 차이는 나타나지 않았다. 신경손상 7일 후 신경손상 모델에서 PKMζ 및 p-PKMζ의 발현량은 대조군의 발현량에 비해 의미있게 증가한 것을 관찰하였다. 이와 같은 결과들은 신경손상에 의해 PKMζ관련 신경가소성이 IC에서 발생할 수 있다는 것을 나타낸다.

세 번째 세부연구는 신경병증성통증 모델의 IC에서 PKMζ가 통증 조절에

관여 할 수 있는 기능적 역할을 확인하기 위해 수행되었다. IC에 ζ-pseudosubstrate inhibitory peptide (ZIP, PKMζ의 선택적 억제제)를 미세주입 후, 기계적 역치 및 PKMζ, p-PKMζ, GluR1 및 GluR2의 발현 수준을 관찰하였다. 기계적 역치는 ZIP microinjection후에 의해 유의미하게 증가되었으며 이와 같은 진통 효과는 12 시간 지속되었다. 또한, GluR1, GluR2 및 p-PKMζ의 발현량은 ZIP 미세주입 후에 감소되었다. 이러한 결과는 ZIP이 신경손상 후에 일어난 IC의 PKMζ관련 신호조절을 통해 통증을 조절할 수 있다는 것을 보여준다.

종합하면, 이러한 결과는 말초 자극에 대한 IC의 높은 흥분성은 신경병증성 통증과 관련이 있으며, 이는 신경 손상 후 IC에서 일어나는 신경가소성이 관여한다는 것을 시사한다. 이러한 변화는 말초 신경 손상에 의해 IC에서 PKMζ와 관련된 신경가소성에 의해 일어나며, PKMζ의 억제제인 ZIP은 만성통증 치료에 적용 가능한 물질로 기대된다.

핵심되는 말: 뇌섬엽, 신경손상, 신경병증성통증, 신경가소성, 인산화효소Mζ

# PUBLICATION LIST

1. Kwak Y, **Han J,** Rhyu MR, Nam TS, Leem JW, Lee BH. Different spatial expressions of c-Fos in the nucleus of the solitary tract following taste stimulation with sodium, potassium, and ammonium ions in rats. J Neurosci Res 2015;93:340-9.
2. **Han J**[*]**,** Kwon M[*], Cha M, Tanioka M, Hong SK, Bai SJ, et al. Plasticity-related PKMζ signaling in the insular cortex is involved in the modulation of neuropathic pain after nerve injury. Neural Plast 2015;601767.
3. **Han J,** Cha M, Kwon M, Hong SK, Bai SJ, Lee BH. In vivo voltage-sensitive dye imaging of the insular cortex in nerve-injured rats. Neurosci Lett 2016;634:146-52.
4. Kwon M[*], **Han J**[*]**,** Kim UJ, Cha M, Um SW, Bai SJ, et al. Inhibition of mammalian target of rapamycin (mTOR) signaling in the insular Cortex alleviates neuropathic pain after peripheral nerve injury. Front Mol Neurosci 2017;10:79.

[*]**These authors have contributed equally.**